

**Materials
Horizons****Review on Organosulfur Materials for Rechargeable Lithium
Batteries**

Journal:	<i>Materials Horizons</i>
Manuscript ID	MH-REV-08-2020-001364.R1
Article Type:	Review Article
Date Submitted by the Author:	08-Oct-2020
Complete List of Authors:	Shadike, Zulipiya; Brookhaven National Laboratory, chemistry division Tan, Sha; Stony Brook University Wang, Qin-chao; Fudan University, Department of Materials Science Lin, Ruoqian; Brookhaven National Laboratory Hu, Enyuan; Brookhaven national lab., ; Brookhaven National Laboratory, Chemistry Department Qu, Deyang; UW Milwaukee, Mechanical Engineering Yang, Xiao-Qing; Brookhaven National Lab, Chemistry

SCHOLARONE™
Manuscripts

Review on Organosulfur Materials for Rechargeable Lithium Batteries

Zulipiya Shadike^{a§*}, Sha Tan^{a§}, Qin-Chao Wang^a, Ruoqian Lin^a, Enyuan Hu^{a*}, Deyang Qu^b, Xiao-Qing Yang^{a*}

^a Chemistry Division, Brookhaven National Laboratory, Upton, NY 11973, USA

^b Department of Mechanical Engineering, College of Engineering and Applied Science, University of Wisconsin Milwaukee, Milwaukee, WI, 53211, USA

§ These authors contributed equally.

Email: zshadike@bnl.gov; enuh@bnl.gov; xyang@bnl.gov

Abstract

Organic electrode materials have been considered as promising candidates for the next generation rechargeable battery systems due to their high theoretical capacity, versatility, and environmentally friendly nature. Among them, organosulfur compounds have been receiving more attention in conjunction with the development of lithium-sulfur batteries. Usually, organosulfide electrodes can deliver relatively high theoretical capacity based on reversible breakage and formation of disulfide (S-S) bonds. In this review, we provide an overview of organosulfur materials for rechargeable lithium batteries, including their molecular structural design, structure related electrochemical performance study as well as electrochemical performance optimization. In addition, recent progress of advanced characterization techniques for investigation of the structure and lithium storage mechanism of organosulfur electrodes are elaborated. To further understand the perspective application, additive effect of organosulfur compounds for lithium metal anodes, sulfur cathodes as well as high voltage inorganic cathode materials are reviewed with typical examples. Finally, some remaining challenges and perspective of the organosulfur compounds as lithium batteries components are also discussed. This review is intended to serve as a general guidance for researcher to facilitate the development of organosulfur compounds.

1. Introduction

Lithium ion batteries (LIBs) using intercalation-type cathode materials such as LiFePO_4 and LiCoO_2 , have a large market share of portable electronics, and electric vehicles due to their high energy density.^{1, 2} However, searching for new generation of rechargeable lithium battery technologies with low cost and better safety characteristics using more environmental friendly and naturally abundant materials is getting more and more attention. In this aspect organic compounds have several advantages comparing with the inorganic electrode materials. First, organic compounds only have light elements such as C, H, O, N, and S, leading to low cost and high gravimetric energy density. Second, structural diversity, flexibility and processability are helpful in designing and synthesizing organic compounds with desired properties. Thirdly, organic compounds can provide multi lithiation sites leading to high energy density. Finally, some alkali metal ions with large ionic radius such as Na^+ and K^+ are difficult to intercalate into inorganic materials but can be utilized in various alkali-ion batteries³⁻⁷ using organic cathode materials. Organic electrode materials can be roughly grouped into several categories, including organosulfur compounds (organosulfide and thioether), conductive polymers, organic radicals, carbonyl compounds and azo compounds. The redox processes, advantages and disadvantages of different organic electrode materials are summarized in table 1. Among them, organosulfides, carbonyl compounds and azo compounds are n-type, in which the neutral state can only be reduced to the negatively charged state, while thioether is p-type organics, in which the

neutral state can only be oxidized to positively charged state (concept of n-type and p-type borrowed from semiconductor). Conductive polymers and organic radicals belong to the bipolar organics, in which the neutral state can be either reduced or oxidized within the different voltage ranges.

Table 1. Redox mechanism, advantages, and disadvantages of different organic electrode materials.

Materials		Redox Mechanism	Advantages	Disadvantages
Organosulfur	Polysulfides	$R-S-S-R' \rightleftharpoons R-S^+ + ^-S-R'$	high capacity and wide operating temperature range	sluggish kinetics high solubility in the electrolyte
	Thioethers	$R-S-R' \rightleftharpoons R-S^+-R'$		
Conductive Polymer		$(-R-)_{\text{n}}^{x+} \xrightleftharpoons{\text{p type}} (-R-)_{\text{n}} \xrightleftharpoons{\text{n type}} (-R-)_{\text{n}}^{y-}$	high conductivity	low capacity
Nitroxyl Radicals		$R-N^+(O)=R' \xrightleftharpoons{\text{p type}} R-N(O)\cdot \xrightleftharpoons{\text{n type}} R-N(O)^-R'$	fast kinetics and flat plateau	high solubility, low capacity and low conductivity
Carbonyl Compounds		$R-C(=O)-R' \rightleftharpoons R-C(O^-)-R'$	fast kinetics and high capacity	low conductivity and high solubility in the electrolyte
Azo Compounds		$R-N=N-R' \rightleftharpoons R-N^--N^--R'$	fast kinetics and stable cyclic life	high solubility and low conductivity

Typical examples of these six different organic electrode materials with their redox mechanisms and cyclic voltammograms can be found in Figure 1.⁸⁻¹³ Usually, compounds with p-type have higher redox potential than those with n-type. For example, conductive polymers, organic radicals and thioethers have redox potential above 3.5 V, while organosulfides, azo compounds and carbonyl compounds have relatively lower redox potential below 3.0 V. Capacity is one of the important factors determining the energy density of the electrodes. Based on the theoretical calculation, organosulfides generally show higher theoretical capacity due to the multi-electron reactions of S-S bonds, which is unique to organosulfides. Azo compounds and carbonyl compounds can also deliver relatively higher capacity than conductive polymers and organic radicals. The capacity of the conductive polymers is limited by the low doping level (usually 0.3-0.5), which is the main drawback of them. Conductivity and kinetics are important factors determining the rate performance and electrochemical polarization. Organosulfur suffers from the sluggish kinetics mostly because the cleavage and recombination of S-S or S=O bonds need a high activation energy. In contrast, organic radicals and conductive polymers show fast kinetics with low voltage polarization and excellent high rate performance. It can be clearly seen from Table 1, that the undesired solubility is one major problem for most of them, especially organosulfur, azo compounds and organic radicals. Generally, organic compounds and their lithiated ones with smaller molecules can hardly avoid dissolution in electrolytes, which is the main reason of capacity decay and poor cyclic life. In comparison, polymers are usually insoluble in the electrolytes and likely to achieve much more stable cycle life. As mentioned above, organosulfur electrodes can provide much higher capacity based on multi-electron redox. At the same time, their low cost, biodegradability, and low toxicity have attracted a lot of attention from researchers.¹⁴⁻¹⁶ More importantly, most of studies on organosulfur electrodes are in conjunction with the development of lithium-sulfur (Li-S) battery, which is one of the most promising power device candidates because of its high theoretical energy density of 2600 Wh kg⁻¹. However, the practical application of Li-S batteries is still impeded by several challenges such as low sulfur utilization as well as the shuttling of the dissolved high-

order lithium polysulfides (Li_2S_x , $4 \leq x \leq 8$).^{17, 18} Tremendous efforts have been made to suppress this. Demobilizing the sulfur by attaching it on the organic backbone has been proved to be an effective way for improving the overall performance of Li-S batteries.¹⁹ Molecularly designed organodisulfides and organopolysulfides not only deliver higher capacity but also show much more stable cyclic performance than elemental sulfur cathodes. For example, sulfurized polyacrylonitrile (SPAN) with a special conjugated structure shows “solid-solid” redox mechanism without polysulfide shuttling, which leads to high sulfur utilization and improved rate performances.²⁰ Moreover, several studies indicated that liquid organosulfur compound such as dimethyl disulfides (DMDS) can be used as a co-solvent/additive for Li-S batteries to enable robust performance of sulfur cathode.²¹ Compared to other organic compounds such as conjugated carbonyl compounds and imide/azo compounds, the research on organosulfur electrodes is still in its early stages. Therefore, a review on the development of the organosulfur electrode materials is quite helpful.

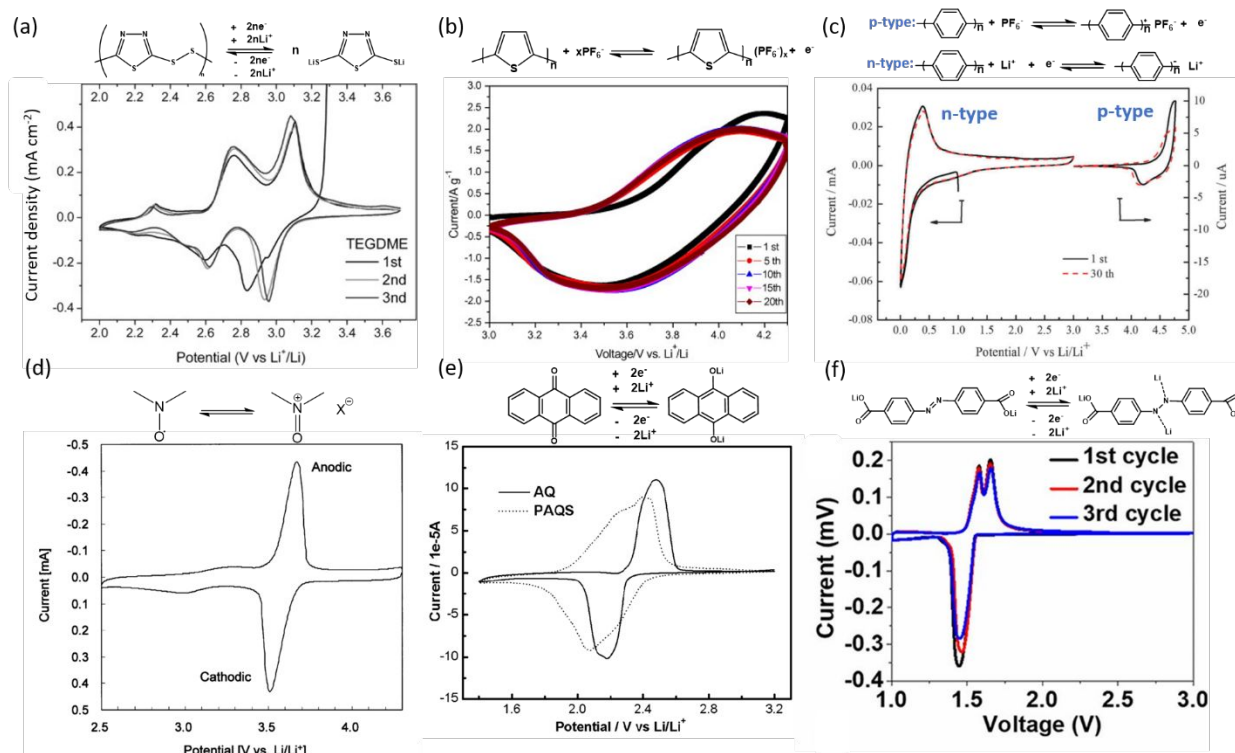


Figure 1. Cyclic voltammograms of (a) poly(2,5-dimercapto-1,3,4-thiadiazole) (PDMcT)/poly(3,4-ethylenedioxythiophene) (PEDOT) composite electrode of 0.05 mV s^{-1} . Reproduced with permission.⁸ Copyright 2012, Wiley-VCH. (b) Li/ Polythiophene (PTH) cell at a scan rate of 10 mV s^{-1} . Reproduced with permission.⁹ Copyright 2012, Elsevier. (c) The polyparaphenylene (PPP) polymer at n-dopable and p-dopable potential regions. Reproduced with permission.¹⁰ Copyright 2013, Royal Society of Chemistry. (d) Poly (2,2,6,6-tetramethylpiperidinyloxy methacrylate) (PTMA) composite electrode at sweep rate of 10 mV/s . Reproduced with permission.¹¹ Copyright 2002, Elsevier. (e) anthraquinone (AQ) and poly(anthraquinonyl sulfide) (PAQS) at a scan rate of 0.1 mV s^{-1} . Reproduced with permission.¹² Copyright 2009, Royal Society of Chemistry. (f) Azobenzene-4,4'-dicarboxylic acid lithium salt (ADALS) electrode at 0.1 mV s^{-1} . Reproduced with permission.¹³ Copyright 2018, National Academy of Sciences.

In this paper, recent development on organosulfur electrode materials is reviewed including three major classes of organodisulfides, organosulfide polymers and thioethers. The development, structural characterization, and optimization of SPAN electrode are summarized separately since it has been

considered as a promising candidate for sulfur cathode. Meanwhile, strategies for optimization of electrochemical performances of organosulfur electrodes are also summarized with typical examples. Furthermore, the role of liquid organosulfur compounds in Li-S and Li metal anode (LMA) batteries and properties of organosulfur compounds as SEI/CEI film-forming additives are discussed. Finally, an outlook about the future development of organosulfur electrode materials and Li-S batteries is also presented.

2. Overview of Organosulfur Electrode Materials

The concept of using organosulfur electrode materials for energy storage was first introduced in 1988 by Visco et al.^{22, 23} They systematically investigated the charge/discharge behavior and ionic conductivity of various organosulfur electrodes such as tetraethylthiuram disulfide (TETD) in sodium battery system. Although such organosulfur electrode showed poor cyclability and large polarization, the advantages of low cost, low toxicity, low corrosivity and low operating temperature make this type of compounds particularly promising for energy storage applications. Since then, more research works have been focusing on the development of novel organosulfur electrodes for lithium batteries. The electrochemical performances of recently developed organosulfur electrode materials categorized in organodisulfides, organosulfide polymers and thioethers are summarized in Table S1. Efforts for molecularly design, structural optimization as well as the electrochemical performance improvement are discussed in detail below.

2.1 Organodisulfide cathode materials

It is well-known that the organodisulfide electrodes has a reversible redox reaction at their disulfide bonds as below: (R is an organic moiety)



In which the capacity is contributed by reversible cleavage and formation of S-S bond during discharge and charging processes. Earliest utilization of organodisulfide electrode in lithium battery was reported by Visco et al.,²⁴ who studied the electrochemistry of Li/TETD battery using an organic solvent electrolyte. Their results showed that Li/TETD system provides a practical energy density of 82 Wh kg⁻¹ at a current density of 16 mA cm⁻², and a stable cyclic performance over 135 cycles was achieved with the depth of charge at 10%, which was not bad for the ambient temperature Li/RSSR cell. However, several critical issues, such as self-discharge, dissolution of active materials as well as instability of LMA needed to be resolved for this system. After that, more studies showed possible utilization of aromatic hydrocarbon contained disulfides as cathode materials for lithium batteries. Inamasu et al.²⁵ investigated the lithium storage properties of phenyl disulfide (DPDS), dibenzo[c,e][1,2]dithiin (DBDT), naphtho[1,8-cd][1,2]dithiol (NDT) and naphtho[1,8-cd:4,5-c'd']bis[1,2] dithiol (NDBT) using polymer electrolyte. Among them, theoretical capacity of NDBT is calculated as 427.7 mAh g⁻¹ based on four electron transfer per formula unit. However, the real capacity of these compounds was rate-dependent with rather poor reversibility. To improve the kinetics and reversibility of DPDS electrode, Bhargav et al.²⁶ prepared a core sheath structured DPDS@ CNT free-standing composite electrode using a simple and scalable phase extraction technique. As shown in Fig. 2a, in the ether based liquid electrolyte, DPDS@CNT electrode delivered a high reversible capacity of 200 mAh g⁻¹ and showed outstanding rate performance when cycled at different rates from C/20 to 3C. This result provides an effective way to increase active material utilization, improve the charge transfer and enhance the overall performance of organodisulfide cathodes.

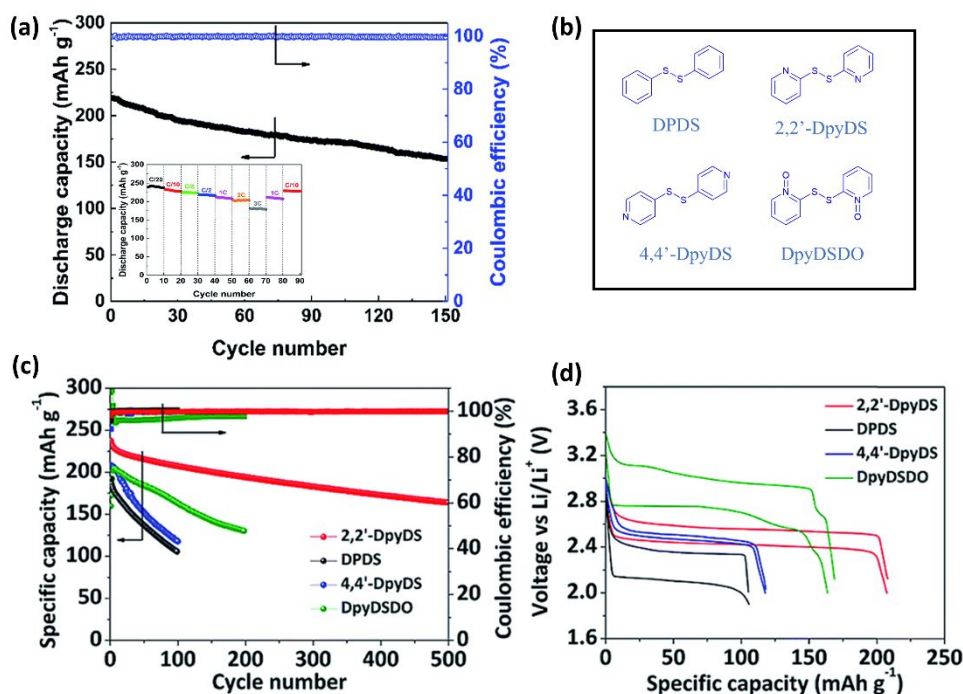


Figure 2. (a) Cycle life of the DPDS@CNT cathode with $\sim 5\text{ mg cm}^{-2}$ loading cycled at 1C and the rate performance of the cathode at different rates demonstrating its fast lithium storage behavior. Reproduced with permission.²⁶ Copyright 2017, Royal Society of Chemistry. (b) Molecule structures and (c) cyclic performances of diphenyl disulfide and dipyridyl disulfides at C/2 rate; (d) The charge/discharge profiles of these cells in the 100th cycle. Reproduced with permission.²⁷ Copyright 2019, Royal Society of Chemistry.

More recently, Fu's group²⁷ further modified the molecular structure of DPDS to investigate the effect of N-containing heterocycles on the electrochemical behavior of organosulfides. In their study, the relationship between molecular structure and electrochemical performances for a series of dipyridyl disulfides (Fig. 2b) with similar capacity was investigated in comparison with DPDS. It can be seen from Fig. 2 c-d that although these disulfides have similar molecular structure, charge/discharge behaviors and cyclic performances are completely different. Among them, DPDS has the lowest working voltage with a large polarization and rapid capacity degradation. In contrast, DpyDSDO has the highest charge/discharge voltages with a slightly increased reversible capacity. However, the cyclic stability of DpyDSDO was still not satisfied. 2,2'-DpyDS, with N atoms on the ortho positions of pyridyl ring showed flat voltage plateau with highest reversible capacity and most stable cyclic performances as well as high coulombic efficiency. These results indicated that when the phenyl group is replaced by the pyridyl ring, the working voltage, energy efficiency as well as the cyclic stability of organosulfides can all be increased. Moreover, their theoretical calculation clearly demonstrated that the outstanding cyclic stability of 2,2'-DpyDS can be attributed to the formation of tight cluster through N-Li-S bridges coordinated by lithium ions, which prevented the dissolution of discharge products. It is well accepted that the conjugated structure facilitates the electron transportation process during the electrochemical reaction and further improves the kinetics of the organosulfides.²⁸ Therefore, organic molecules with disulfide bonds and conjugated backbone has become an emerging topic. Xue et. al.²⁹ attempted to stabilize four disulfide bonds to a large conjugated system. They synthesized anthra[1',9',8'-b,c,d,e][4',10',5'-b',c',d',e']bis-[1,6,6a(6a-S^{IV})trithia]pentalene (ABTH) as a cathode for lithium battery, in which disulfide bonds are connected to three conjugated benzene rings with theoretical capacity of over 400 mA h g⁻¹ based on 6-electron redox reaction. However,

this conjugated disulfide electrode only delivered an initial capacity of 125 mAh g⁻¹ at 10 mA g⁻¹ current rate using carbonate-based electrolyte and after 7 cycles, the capacity decreased to ~100 mAh g⁻¹ which was only 25% of the theoretical capacity. This result demonstrated one critical issue of organodisulfide electrode: the dissolution of the monomer and/or discharge products into the electrolyte, which is the main reason of the capacity decay. To improve the charge-discharge stability and increase the electronic conductivity of ABTH, the homopolymer of ABTH was synthesized by oxidative coupling reaction. As expected, polymerized PABTH showed improved conductivity of 10⁻² S cm⁻¹ and delivered much higher reversible capacity of 300 mAh g⁻¹. Later, to systematically investigate the capacity degradation mechanism of PABTH, Li et al.³⁰ compared the cyclic stability of PABTH electrodes in ether and carbonate-based electrolytes. As shown in Fig. 3a-b, PABTH electrode in lithium bis(trifluoromethanesulfonyl)(LiTFSI)-dioxolane(DXL)-dimethoxyethane(DME) electrolyte showed higher reversible capacity with better cyclic stability than that of in the LiClO₄-ethylene carbonate (EC)-dimethyl carbonate (DMC) electrolyte, demonstrated that the electrochemistry of organodisulfides strongly relates to the electrolyte and the ether based electrolyte may suppress dissolution of the organodisulfides.

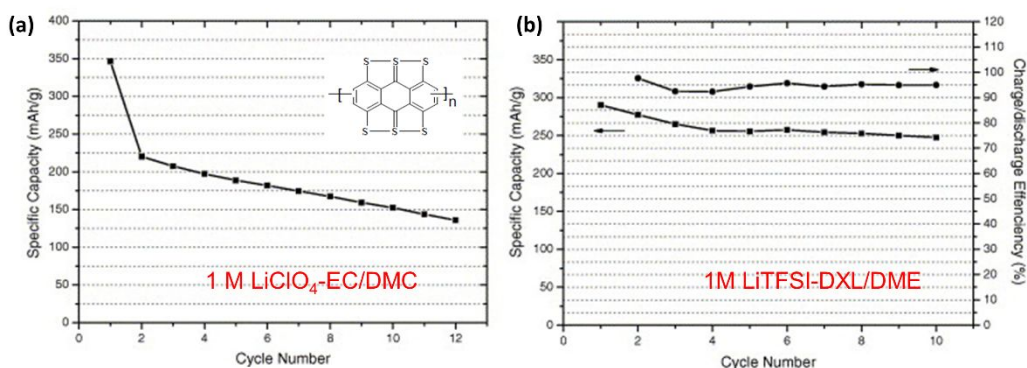


Figure 3. Cycling life of PABTH cycled at 20 mA g⁻¹ in (a) 1 M LiClO₄-EC/DMC (1:1 by volume) and (b) 1M LiTFSI-DXL/DME (2:1 by weight) electrolytes. Reproduced with permission.³⁰ Copyright 2007, Elsevier.

Many studies showed that polymerization of the organodisulfides can effectively inhibit the loss of sulfur species into the electrolyte during cycling. Two types of organodisulfide polymers, main-chain type and side-chain type, have been investigated. In the former one, disulfide bonds are located in the main polymer chain and cleavage/regeneration takes place in the main polymer chain during discharge/charge, while in the latter one the disulfides are attached to the side chain of the polymer backbone. It is easy to understand that main-chain type disulfide polymer reduces to thiolate ions during discharge process and they are soluble in most of organic liquid electrolytes. At the same time, the inner polymer disulfide bond does not offer high rejoining efficiency due to their sluggish kinetics, leading to low coulombic efficiency and severe capacity degradation. A representative example is 2,5-dimercapto-1,3,4-thiadiazole (DMcT)-one of the widely investigated organodisulfide electrode with a high theoretical capacity of 362 mAh g⁻¹.³¹⁻³³ As shown in Fig. 4a, poly (2,5-dimercapto-1,3,4-thiadiazole) (PDMcT) can be depolymerized to lithiated-DMcT monomer during the discharge process. However, such a lithiated product is soluble in the organic electrolyte and repolymerization of DMcT to PDMcT has very poor kinetics. Doeff et al.³⁴ prepared thin film lithium polymer electrolyte to study the electrochemical behavior of PDMcT at 90-100 °C and provided an experimental evidence for the feasibility of using PDMcT as cathode material for lithium battery. Their result showed that PDMcT cathode can be discharged at a high rate of C/2 with 80% of active material utilization. Since then, efforts have been made to improve the cyclic stability of PDMcT in liquid electrolyte at room temperature. Reports on coating PDMcT by conductive polyaniline (PAN) or polypyrrole (PPy)

further promoted the development of PMDcT cathode material.³⁵⁻³⁷ Oyama et al.³⁵ prepared PAn coated PMDcT by molecular-level mixing and successfully improved the active material utilization with about 80% utilization of active material and capacity retention of 80% after 100 cycles. To improve the conductivity of PMDcT, Li et al.³⁶ prepared a conductive PMDcT/PPy composite thin film via surfactant template technique and investigated the electrochemical properties of them. Although conductivity of PMDcT was increased from $5.9 \times 10^{-13} \text{ S cm}^{-1}$ to $2.91 \times 10^{-3} \text{ S cm}^{-1}$ with PPy coating, dissolution of DMcT into the electrolyte was not suppressed. Poly(3,4-ethylenedioxythiophene) (PEDOT) coating have also showed the ability to accelerate the redox reaction of PMDcT electrode.^{8, 38, 39}

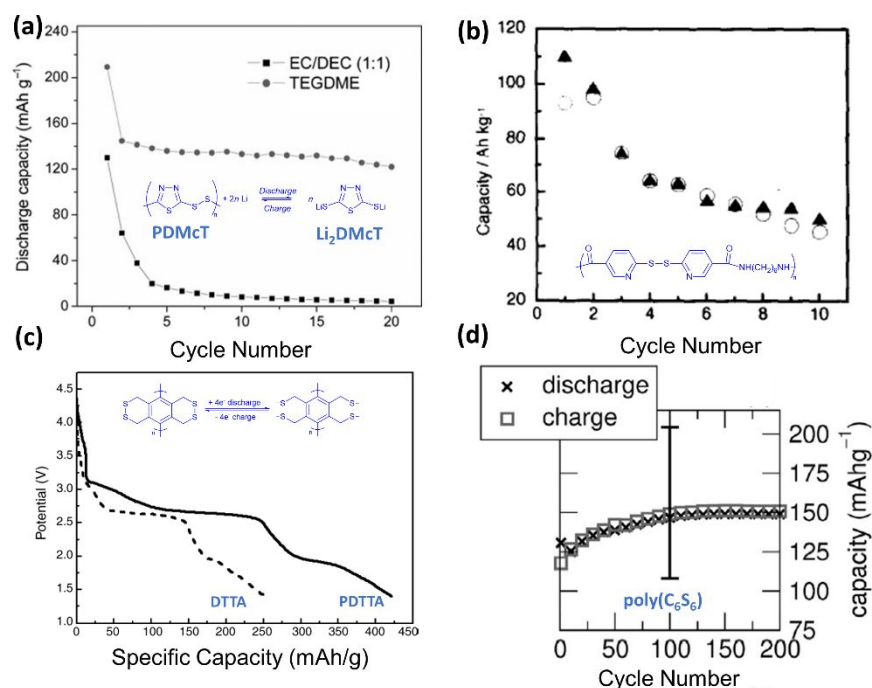


Figure 4. (a) Comparison of cycle performance of PMDcT/PEDOT composite between LiPF₆ (1.0 M) in EC/DEC (1:1 by volume) and LiPF₆ (1.0 M) in TEGDME. Inset shows redox process of PMDcT. Reproduced with permission.⁸ Copyright 2012, Wiley-VCH. (b) Variation in capacity of 6,6'-Dithiodinicotinic acid and polyamide estimated from the cathodic peak area of *cv* with cycling number. Reproduced with permission.⁴¹ Copyright 1996, Elsevier. (c) The second cycle of discharging curve for: DTTA and PDTTA in 1.0M LiClO₄-EC/DMC (1:1, v/v) at a current density of 30 mA g⁻¹. Reproduced with permission.⁴³ Copyright 2006, Elsevier. (d) Cycling performance of poly(C₆S₆) at current rate of C/10 cycled within 1.0-3.0V. Reproduced with permission.⁴⁵ Copyright 2017, Wiley-VCH.

In the study reported by Gao et al.⁸, PMDcT/PEDOT composite electrode showed an initial capacity of 210 mAh g⁻¹ in the ether-based electrolyte and the capacity still remained around 120 mAh g⁻¹ after 20 cycles (Fig. 4a). These examples demonstrated that, when coated or composited with other organic compounds such as conductive polymers, the overall performance of organodisulfides can be significantly improved. Nitrogen in the aniline or pyridine can improve the ion conductivity of polymer electrodes. Polyamides containing organodisulfides polymers were first investigated by Tsutsumi et al.^{40, 41} They reported the synthesis process and electrochemical properties of the polyamides that have alkyl chain backbone and disulfide bond⁴¹ and further optimized the structure by introducing the aromatic polyamides in the main chain. They suggested that the amide group can decrease the solubility of dithiol formed during discharge process. As a result, when using the LiClO₄/acetonitrile (AN) electrolyte, the compound shown in Fig. 4b

delivered an initial capacity of 93 mAh g⁻¹, which is 67% of the theoretical capacity. Although, the kinetics was improved by introducing various conductive polymer backbone, the cyclic stability was not improved as expected. Scientists therefore turned their attention to the polymers with disulfide bond on the side chain of polymer. In comparison, side chain organodisulfide polymers can effectively maintain the backbone structure even after disulfide bond is broken, resulting in long cycle life and high coulombic efficiency. Sulfurized polyacrylonitrile (SPAN) cathode is the most successful example of side-chain type disulfide compounds. Its electrochemical optimization and structural modification will be discussed later. Poly-2,2'-Dithiodianiline (PDTDA) is another well-known organodisulfide polymer electrode, which is a conducting polymer with disulfide bond.⁴² An electroactive thin film was formed by electrochemically polymerization of DTDA. The novel poly (DTDA) showed enhanced redox reactions with a high capacity of 270 mAh g⁻¹ due to an intramolecular electrocatalytic effect of aniline/anilinium and thiol/thiolate redox couples. Benzene-based polyorganodisulfide derivatives usually have high disulfide content connected with polyphenyl with higher theoretical capacity over 400 mAh g⁻¹, which can enhance the redox of the S-S bond. The most promising advantage is that the intramolecular cleavage/recombination of disulfide bond resulted in the higher recombination probability of S-S bond than the intermolecular one. At the same time, conjugated structure of the polymer backbone is beneficial for electron transfer. As an example, Deng et al.⁴³ designed and synthesized a novel benzene-based polydisulfide, poly(5,8-dihydro-1H,4H-2,3,6,7-tetrathia-anthracene) (PDTTA) as a cathode material for lithium battery. As shown in Fig. 4c, PDTTA has two six-membered cycles and two S-S bonds, which provides a high theoretical capacity of 471 mAh g⁻¹. PDTTA cathode delivered an initial discharge capacity of 422 mAh g⁻¹ with three discharge plateaus at 3.1, 2.6 and 1.9 V in the carbonate-based electrolyte. Compared to the poor performance of DTTA monomer with 257 mAh g⁻¹ capacity for the initial cycles and 29 mAh g⁻¹ after 44 cycles, the side-chain organodisulfide polymer PDTTA did improve the cyclic stability (170 mAh g⁻¹ after 44 cycles). Tetrathionaphthalene (TTN), a naphthalene derivative with two S-S bonds, possesses 4-electron transfer process during electrochemically redox. However, when disulfide bonds are cleaved, four thiolate groups formed, these are highly soluble in the electrolyte, resulted in poor reversibility. Sarukawa et al.⁴⁴ employed thioether linkages between TTN molecules and synthesized sulfur-linked TTN polymer (poly(S-TTN)). Thioether in this polymer not only links TTN polymer to prevent their dissolution, but also provides extra capacity when appropriated voltage range is applied. Results showed a stable cyclic performance over 180 cycles between 3.2-4.4 V, but irreversible reaction occurred when cycled over 4.5 V. The irreversible process over 4.5 V was attributed to the oxidation of linkage sites, leading severe capacity degradation. Electrochemical performance of other side chain organodisulfide polymers is summarized in Table 1, showing that side chain organodisulfide polymers have much improved cyclic stability and kinetics compared to the main-chain type ones. More recently, a cross-linked polydisulfide with phenyl rings was studied as a highly stable cathode material for lithium battery by Preefer et al.⁴⁵ In which, each C₆S₆ monomer contained 50 mol% of S and 50 mol% of C, this value is close to the S content in the carbon-sulfur composite electrodes previously studied. Theoretical capacity of poly (C₆S₆) is 609 mAh g⁻¹ based on 6 electron-transfer per monomer, which is the highest value among the polydisulfide electrodes reported but not all disulfide bonds were utilized in reality. However, thanks to the stable cross-linked structure, poly(C₆S₆) electrode showed very stable cyclic performance over 200 cycles with 98% capacity retention in ether-based electrolyte as shown in Fig. 4d. Combining the advantages of different organic groups also provided an effective strategy to improve the kinetics and cyclability of organodisulfide materials. Shadike in Yang's group⁴⁶ designed and synthesized a novel organodisulfide compound, 2,3,4,6,8,9,10,12-Octathia bicyclopenta [b,c]-5,11-anthraquinone-1,7-dithione (TPQD), and systematically investigated its electrochemical properties and charge storage mechanism. A benzoquinone coordinated with dithiolane through 1,4-dithianes not only provides extra capacity, but also facilitates better kinetics of disulfide bond due to its π -conjugation. TPQD electrode delivered capacity of 251.7 mAh g⁻¹ with a high coulombic

efficiency of 91.7% at the initial cycle and relatively stable cyclic performance at the current rate of C/10. More impressive performances were achieved at high rate of 5C, a reversible capacity of 130 mAh g⁻¹ was retained for 200 cycles with a slow capacity decay rate of 0.07% per cycle.

Although organodisulfide compounds have high theoretical capacity, the practical capacity is still not satisfactory. Further development of organosulfur cathode needs to consider the active sulfur content in the molecule. Usually, the sulfur content in organosulfur compounds can be increased by manipulating the disulfide unit, such as organotrissulfide (RSSSR) and organotetrasulfide (RSSSSR) compounds with two or three S-S. Organosulfur compounds based on multiple S-S bonds are first introduced by Naoi et al.⁴⁷ to increase the energy density. The energy density of organosulfide electrode materials increases with the number of the S-S bond in the structure, as exemplified by poly DMcT-disulfide, poly DMcT-trisulfide and poly DMcT-tetrasulfide electrodes. As the number of S-S bond increased, the discharge capacity increased from 150 mAh g⁻¹ for disulfide polymer to 280 mAh g⁻¹ for the tetrasulfide polymer. However, cyclic performances were not investigated for these polymers.

In recent years, various organotrissulfide and tetrasulfide compounds were designed and synthesized by Fu's group and successfully utilized as cathode material for lithium batteries. Liquid dimethyl trisulfide (DMTS, CH₃SSSCH₃), has a theoretical capacity of 849 mAh g⁻¹ with four electro redox reaction, can form catholyte with electrolyte. Fu's group⁴⁸ used binder-free multi-walled carbon nanotube (MWCNT) paper as current collector for absorbing DMTS and charged/discharged products. One Li₂S and two lithium thiomethoxides (LiSCH₃) formed during lithiation process as shown in Fig. 5a with capacity of 720 mAh g⁻¹, which is about 80% of the theoretical capacity. After 50 cycles, DMTS electrode still showed a discharge capacity of 590 mAh g⁻¹, corresponding to 82% of the initial capacity. They investigated the capacity degradation mechanism by various characterization methods and found that surface of LMA is passivated by sulfur containing species, indicating the polysulfide shuttling occurs in DMTS cathode. Later, they also reported the electrochemical performance of diphenyl trisulfide (DPTS), in which electron withdrawing group in phenyl is expected to enable higher working potential than DMTS.⁴⁹ As presumed, two cathodic peaks at 2.2 and 2.0V were observed from the discharge plateau of DPTS and most of capacity was obtained from higher voltage region, which was higher than the voltage of DMTS. Although the reversible capacity of DPTS (398 mAh g⁻¹) was lower than that of DMTS due to the higher molecular weight of phenyl, DPTS exhibited better cyclic stability and rate performance due to its stable backbone and low volatility of phenyl group (Fig. 5b). It is worth to mention that a higher energy density of 158 Wh L⁻¹, was achieved when the loading amount of DPTS increased to 7.7 mg cm⁻², which is even higher than most of flow batteries. To further increase the energy density, Guo et al.⁵⁰ comprehensively studied a series of phenyl tetrasulfides (PTS) as cathode, possessing 6 electron redox reaction, for lithium batteries. The physical and electrochemical properties of PTS were tuned by attaching different functional groups, such as electron-donating group OCH₃ and electron-withdrawn group CF₃. Interestingly, p-trifluoromethylphenyl tetrasulfide (CF₃PTS) and p-methoxyphenyl tetrasulfide (CH₃OPTS) showed completely different electrochemical performances although both have similar charge discharge curves. The working potential was in the order of CH₃OPTS < PTS < CF₃PTS, which is consistent with the electron accepting ability of OCH₃, H and CF₃ groups. While, the specific capacity was in the order of CF₃PTS < CH₃OPTS < PTS due to the larger molecule weight of CF₃ and CH₃O groups. As shown in Fig. 5c, the best cyclic stability was obtained for CH₃OPTS with capacity retention of 81% after 100 cycles compared to PTS (74%) and CF₃PTS (43%). Moreover, CH₃OPTS also showed lowest overpotential among these three tetrasulfides. In addition to introducing different functional groups, Se doping is also an effective approach to improve the cyclic stability and rate performance of DPTS electrode. Lithium storage performance and mechanism of DPTS-Se organic-inorganic hybrid material were reported by Zhao et al.⁵¹ The initial discharge capacity of such a hybrid cathode was about 96.5 % of the theoretical value and capacity retention was much improved

comparing with DPTS electrode. Spectroscopic characterization and molecular dynamic analysis results demonstrated formation of dynamic S-Se covalent bonds upon charging, which reduces the formation of soluble lithium polyselenides and lithium polysulfides. These results provided valuable insights and guidance to optimize the electrochemical properties by tuning the molecule structure of organosulfides. Based on their theoretical calculation and characterization results, reduction process of phenyl tetrasulfide electrode can be summarized as schematics shown in Fig. 5d.

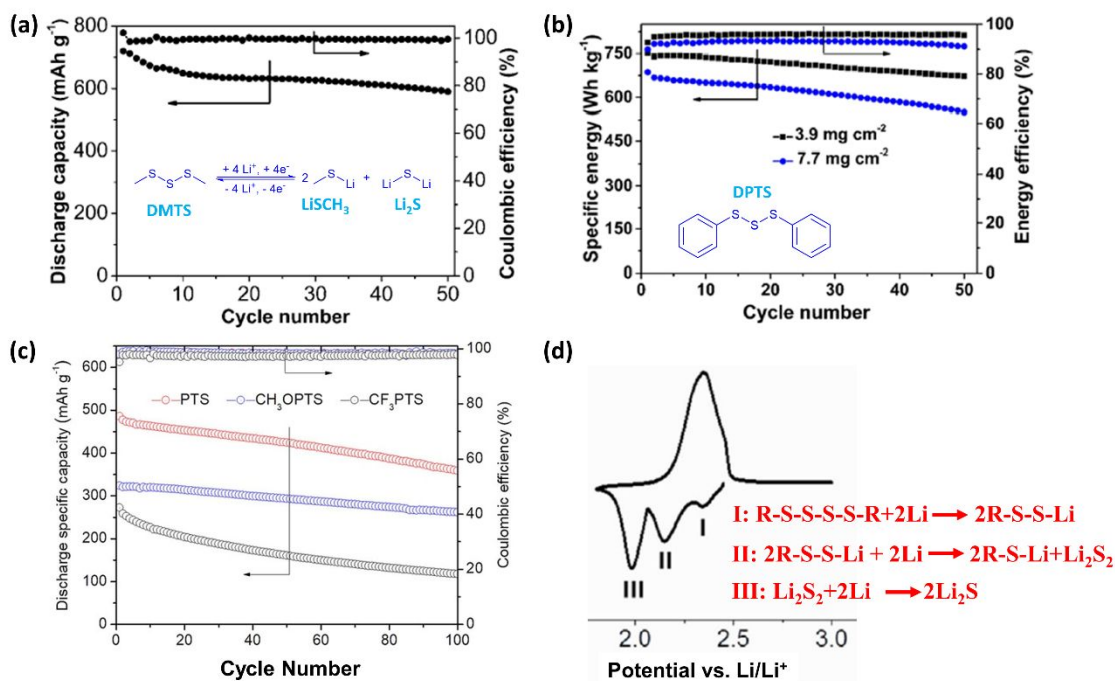
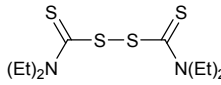
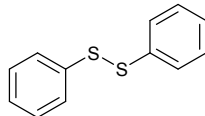
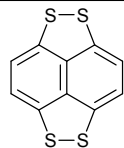
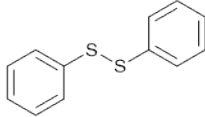
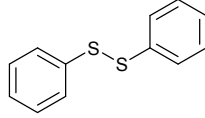
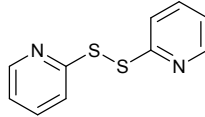
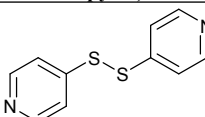
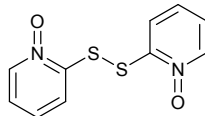
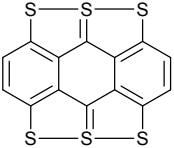
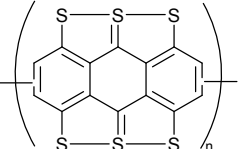
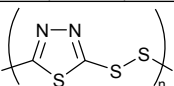
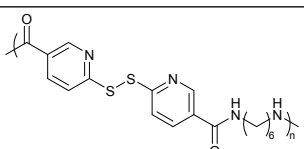
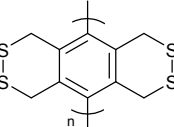
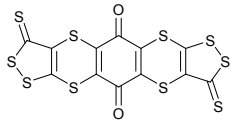
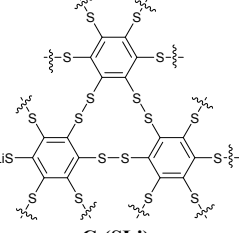
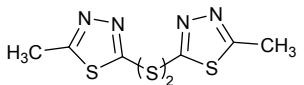


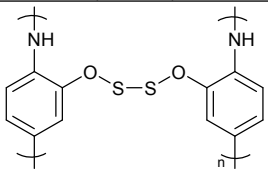
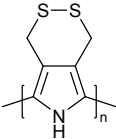
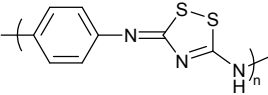
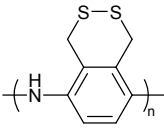
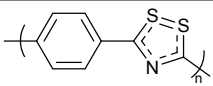
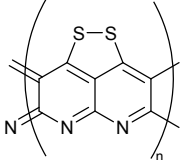
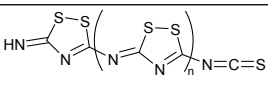
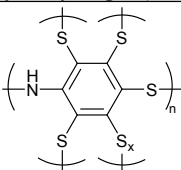
Figure 5. (a) Cyclic performance of DMTS electrode at a current rate of C/10 and its electrochemical mechanism. Reproduced with permission.⁴⁸ Copyright 2016, Wiley-VCH. (b) Molecular structure of DPTS and its cyclic performances with different cathode loading amount at current rate of C/10. Reproduced with permission.⁴⁹ Copyright 2016, American Chemical Society. (c) Cyclic performances of three different diphenyl tetrasulfides: PTS, CH_3OPTS and CF_3PTS with 0.5 M catholytes at C/10. (d) Typical cyclic voltammetry (CV) curve of PTS and schematics of reduction reaction process. Reproduced with permission.⁵⁰ Copyright 2017, Wiley-VCH.

Table 2. Molecular structure and electrochemical performances of organosulfur electrode materials.

Materials	Theoretical Capacity (mAh g ⁻¹)	Specific Capacity (mAh g ⁻¹) / Current density (mA g ⁻¹) or C rate	Capacity retention (mAh g ⁻¹)/cycle number/ current density (mA g ⁻¹)	References Notes
 Tetraethyl thiuram disulfide (TETD)	181 mAh g ⁻¹	82 Wh kg ⁻¹ / 16 mA cm ⁻² (1.7-3.7V)	N/A	²⁴ Liquid electrolyte
 Diphenyl disulfide (DPDS)	245 mAh g ⁻¹	~15/40 mA g ⁻¹ (1.5-3.7 V)	N/A	²⁵ Polymer electrolyte
 Naphtho[1,8-cd:4,5-c'd']bis[1,2] dithiol (NBDT)	425 mAh g ⁻¹	350/20 mA g ⁻¹ 424/8 mA g ⁻¹ (1.5-3.7 V)	N/A	
 Diphenyl disulfide (DPDS)@ (Carbon nanotube)CNT	245 mAh g ⁻¹	218/245 mA g ⁻¹ (1.8-2.8 V)	153/150/245 mA g ⁻¹	²⁶ LiTFSI-DME/DOL (1:1v/v) + 0.2 M LiNO ₃
 DPDS	245 mAh g ⁻¹	193/0.5C (2.0-3.0 V)	104/100/0.5C	²⁷ LiTFSI-DME/DOL (1:1v/v) + 0.2 M LiNO ₃
 2,2'-dipyridyl disulfide (2,2'-DpyDS)	243 mAh g ⁻¹	237/0.5C (2.0-3.0 V)	163.5/500/0.5C	
 4,4'-dipyridyl disulfide (4,4'-DpyDS)	243 mAh g ⁻¹	208/0.5C (2.0-3.0 V)	118.5/100/0.5C	
 2,2'-dipyridyl disulfide-N,N'-dioxide (DpyDSDO)	212 mAh g ⁻¹	160/0.5C (2.0-3.4 V)	131/200/0.5C	
	>400mAh g ⁻¹	125/10 mA g ⁻¹ (1.8-4.5 V)	~100/7/10 mA g ⁻¹	²⁹ LiClO ₄ -EC/DMC (1/1)

 <p>Anthra[1',9',8'-b,c,d,e][4',10',5'-b',c',d',e']bis-[1,6,6a(6a-S^{IV})trithia]pentalene (ABTH)</p>		290/20 mA g ⁻¹ (1.7-2.7 V)	190/11/20 mA g ⁻¹	³⁰ LiTFSI-DXL/DME (2:1, wt%)
 <p>Polyanthra[1',9',8'-b,c,d,e][4',10',5'-b',c',d',e']bis-[1,6,6a(6a-S^{IV})trithia]pentalene (PATBH)</p>	>400mAh g ⁻¹	270/10 mA g ⁻¹ (1.5-4.6 V)	~235/7/10 mA g ⁻¹	²⁹ LiClO ₄ -EC/DMC (1/1)
		290/20 mA g ⁻¹ (1.7-3.3 V)	250/10/20 mA g ⁻¹	³⁰ LiTFSI-DXL/DME (2:1, wt%)
 <p>Poly(2,5-dimercapto-1,3,4-thiadiazole) (PDMcT)</p>	362 mAh g ⁻¹	205/0.1C (2.0-3.7 V)	50/10/0.1C	³⁸ LiBF ₄ -EC/DEC (1:3v/v)
		130/20 mA g ⁻¹ (2.0-3.7 V)	40/3/20 mA g ⁻¹	⁸ LiPF ₆ -EC/DEC (1:1v/v)
		210/20 mA g ⁻¹ (2.0-3.7 V)	120/20/20 mA g ⁻¹	⁸ LiPF ₆ -TEGDME
	138 mAh g ⁻¹	93/NA	45/10/NA	⁴¹ 0.1M LiClO ₄ -AN
 <p>Poly(5,8-dihydro-1H,4H-2,3,6,7-tetrathiaanthracene) (PDTTA)</p>	471 mAh g ⁻¹	422/30 mA g ⁻¹ (1.1-4.4 V)	170/44/30 mA g ⁻¹	⁴³ 1.0M LiClO ₄ -EC/DMC (1:1 v/v)
 <p>2,3,4,6,8,9,10,12-Octathia biscyclopenta[b,c]-5,11-anthraquinone-1,7-dithione (TPQD)</p>	324 mAh g ⁻¹	251.7/32.4 mA g ⁻¹ 212/642 mA g ⁻¹ (1.4-3.5V)	152/100/642 mA g ⁻¹ 120/200/1605 mA g ⁻¹	⁴⁶ 1.0M LiTFSI-DOL/DME (1:1 v/v)
 <p>C₆(SLi)₆</p>	609 mAh g ⁻¹	125/61 mA g ⁻¹ (1.0-3.0V)	150/200/61 mA g ⁻¹	⁴⁵ 1.0M LiTFSI-DOL/DME (1:1 v/v)
 <p>poly DMcT-disulfide</p>	205 mAh g ⁻¹ (2 e ⁻)	150/0.1 mA cm ⁻² (2.0-2.8V)	N/A	⁴⁷ Polyacrylonitrile film containing LiCF ₃ SO ₃ -EC/PC (1:1)

<p>poly DMcT-trisulfide</p>	362 mAh g ⁻¹ (4 e ⁻)	245/0.1 mA cm ⁻² (2.0-2.8V)	N/A	
<p>poly DMcT-tetrasulfide</p>	493 mAh g ⁻¹ (6 e ⁻)	280/0.1 mA cm ⁻² (2.0-2.8V)	N/A	
<p>Dimethyl trisulfide (DMTS) on MWCNT</p>	849 mAh g ⁻¹	720/84 mA g ⁻¹ (1.7-2.7V)	590/50/84 mA g ⁻¹	⁴⁸ 1M LiTFSI-DME/DOL (1:1v/v) + 0.1 M LiNO ₃
<p>Nominal diphenyl trisulfide (DPTS)</p>	428 mAh g ⁻¹	398/428 mA g ⁻¹ 330/214 mA g ⁻¹ (1.8-2.7 V)	260/100/214 mA g ⁻¹	⁴⁹ LiTFSI-DME/DOL (1:1v/v) + 0.1 M LiNO ₃
<p>Phenyl tetrasulfide (PTS)</p>	569.3 mAh g ⁻¹	486/57 mA g ⁻¹ (1.8-3.0 V)	360/100/57 mA g ⁻¹	⁵⁰ 1M LiTFSI-DME/DOL (1:1v/v) + 0.2 M LiNO ₃
<p>P-methoxyphenyl tetrasulfide (CH3OPTS)</p>	469.5 mAh g ⁻¹	324/47 mA g ⁻¹ (1.8-3.0 V)	262/100/47 mA g ⁻¹	
<p>P-trifluoromethylphenyl tetrasulfide (CF₃PTS)</p>	384.3 mAh g ⁻¹	272/38 mA g ⁻¹ (1.8-3.0 V)	117/100/38 mA g ⁻¹	
<p>1,2-bis(thiophen-3-ylmethyl)disulfane</p>	209 mAh g ⁻¹ (2 e ⁻)	50/50 mA g ⁻¹ (1.0-4.0 V)	230/20/50 mA g ⁻¹	⁵² 1M LiPF ₆ -Ethyl Cellulose/DEC (1:2, wt%)
<p>PDTA</p>	169 mAh g ⁻¹	113.3/5 mA g ⁻¹ (1.3-4.0 V)	~48/15/5 mA g ⁻¹	⁵³ 1M LiClO ₄ -PC/DME (1:1, v/v)
<p>GTA</p>	185 mAh g ⁻¹	134.7/5 mA g ⁻¹ (1.3-4.0 V)	~37/15/5 mA g ⁻¹	
<p>LiClO₄/EC-PC (1 :1)/polyacrylonitrile-based gel electrolyte</p>	330 mAh g ⁻¹	270/0.1 mA cm ⁻² (2.0-4.0 V)	N/A	⁴²

<p>Poly(2,2'-dithiodianiline) (PDTDA)</p>  <p>Poly[bis(2-aminophenoxy)disulfide] (PAPOD)</p>	261 mAh g ⁻¹	230/0.1 mA cm ⁻² (1.0-3.7 V)	60/7/0.1 mA cm ⁻²	54 1 M LiClO ₄ /PC-EC (1:1, v/v)
 <p>Ploy(4,6-dihydro-1H-[1,2]dithiino[4,5-c]pyrrole) (PolyMPY)</p>	398 mAh g ⁻¹	398/7.88 mA g ⁻¹ (2.0-4.0 V)	30/30/7.88 mA g ⁻¹	55 1M LiClO ₄ -PC
 <p>Poly(p-phenylene thiuret) (PPT)</p>	259 mAh g ⁻¹	259/ 0.07 mA cm ⁻² (1.75-4.5 V)	Charge: 210/4/0.07 mA cm ⁻² Discharge: 259/5/0.07 mA cm ⁻²	56 1 M LiClO ₄ /EC-DEC
 <p>poly(α, α'-dithio-3-amino-o-xylene) (PDTAn)</p>	370 mAh g ⁻¹	225/10 mA g ⁻¹ (1.5-4.7 V)	N/A	57 1 M LiClO ₄ /EC-DMC (1:1,v/v)
 <p>poly(1,4-phenylene-1,2,4-dithiazol-3',5'-yl) (PPDTA)</p>	452 mAh g ⁻¹	420/0.1 mA cm ⁻² (cutoff: 1.75V)	N/A	58 1 M LiClO ₄ /EC-DEC
 <p>Polythiopyrrole (PTP)</p>	327 mAh g ⁻¹	520/0.2 mA cm ⁻² (1.0-3.0 V)	480/240/0.2 mA cm ⁻²	59 1 M LiPF ₆ -EC/DMC (1:1, v/v)
 <p>Polythiocyanogen (SCN)_x</p>	462 mAh g ⁻¹	Discharge: 250/0.2C Charge: 229/0.2C (0-2.0 V)	Discharge: 208/20/0.2C Charge: 201/20/0.2C	60 1.0 M LiPF ₆ in EC-DMC (1:1, wt%)
 <p>Polyaniline polysulfide (SPAN)</p>	1067 mAh g ⁻¹	980/0.1 mA cm ⁻²	403/20/0.1 mA cm ⁻²	61 1M LiCF ₃ SO ₃ /DOL-DME (1:1, v/v)

2.2 Sulfurized polyacrylonitrile (SPAN) electrode materials

SPAN was firstly reported by Wang et al. in 2002. They prepared SPAN with sulfur content of 53.4% simply by heating a mixture of PAN powder and sulfur at 280-300 °C under argon gas protection.⁶²⁻⁶⁴ As a cathode material, SPAN delivered a capacity about 860 mAh g⁻¹ in the initial cycle and 600 mAh g⁻¹ after 50 cycles. Such a higher reversible capacity with high sulfur utilization and relatively stable cyclic performance of SPAN compared to elemental sulfur made it a promising candidate for Li-S batteries. They proposed that -CN group cyclized at melt state of sulfur (at 300°C), resulting in a stable π -conjugated co-plane heterocyclic compound and sulfur remains in elemental state without any C-S bond formation. However, only limited information about the structure of the as-prepared SPAN and its charge storage mechanism were provided in these studies. Afterward, Yu et al.^{59, 65} provided a different structural information through comprehensively characterization of the chemical and physical properties of SPANs prepared at different temperatures. They suggested that cleavage of S8 ring and formation of sulfur-free radicals occur at relatively high temperature. At the same time, other reactions between sulfur and carbon in PAN may also take place. The most important finding of their study is about the C-S and S-S bonding which is confirmed by Fourier-transform infrared spectroscopy (FT-IR), Raman spectroscopy and X-ray Photoelectron Spectroscopy (XPS). Their results showed that SPAN synthesized at relatively lower temperature of 250 °C only contains elemental sulfur or poly(sulfur). However, elemental sulfur is absent in the samples synthesized at higher temperatures of 300, 450 and 800 °C. Moreover, the major structural order of SPANs synthesized above 300 °C showed a graphite-like π -stacking of the hexahydric-ring layer. SPAN electrodes synthesized at different temperatures also have completely different electrochemical properties. Among them, SPAN synthesized below 250 °C was not electrochemically active due to the incomplete reaction between S and PAN. On the other hand, SPANs prepared at 300, 450, 800 °C delivered the initial capacities about 550, 500 and 100 mAh g⁻¹, respectively as shown in Fig. 6a. SPAN synthesized at 450 °C showed the best cycle stability with capacity retention of 92% after 240 cycles. In contrast, severe capacity degradation was observed for that prepared at 300 °C. Excellent cyclic stability of SPAN synthesized at 450 °C was attributed to the good electrical conductivity provided by the π -conjugated structure (Fig. 6a) and the stable back bone structure. Another different molecular structure of SPAN was elucidated by Fanous et al. They investigated the structure of SPAN using time-of-flight secondary ion mass spectrometry (TOF-SIMS), XPS and FT-IR.⁶⁶ By combining different characterization methods, it was suggested that all sulfur atoms in this SPAN are bonded to the polymer backbone, which is consistent with the conclusion of Yu⁵⁹. Sulfur in this SPAN also exists in the form of disulfide, trisulfide and polysulfides, 2- pyridylthiolates as well as thioamide structure as shown in Fig. 6b. Electrochemical performance of SPAN was investigated in ether and carbonate-based electrolytes to understand the role of different electrolytes when oligo(sulfur)s are in the structure. Results in Fig. 6c show that SPAN cycled in ether-based electrolyte has a rapid capacity drop due to the polysulfide shuttle effect. In contrast, stable cyclic performance with little capacity decay was observed in carbonate-based electrolyte containing either LiPF₆ or LiTFSI.

More recently, a new take on the structure and the redox mechanism of SPAN was proposed by Wang et al. using nuclear magnetic resonances (NMR), electron paramagnetic resonance (EPR), and theoretical calculation.²⁰ They proposed that during the charge-discharge process, a conjugative structure can react with lithium ions and form an ion-coordination bond reversibly, which is shown in Fig. 6d. These conclusions, which are different from those reported before, was further confirmed by the superior cyclic stability of SPAN over 2000 cycles with capacity retention of 98.7% in carbonate-based electrolyte, indicating the absence of polysulfide shuttling during the charge-discharge process. They confirmed that the lithiation of SPAN follows the pathway I shown in Fig. 6d, due to the lowest potential energy. In which, thiyl radicals was generated after cleavage of S-S bond in the first cycle, and then conjugated structure formed through electron delocalization of thiyl radical on pyridine backbone. During the charge process,

ionic SPAN converted to radical SPAN rather than returning to the initial molecule, causing different discharge behaviors observed in the first and second cycles.

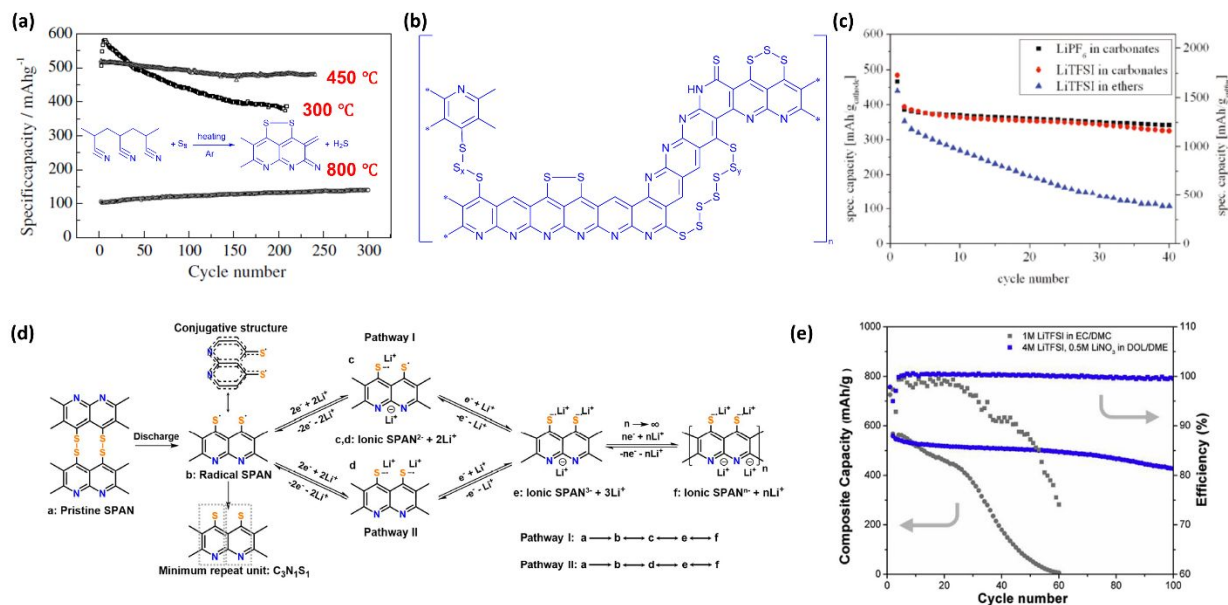


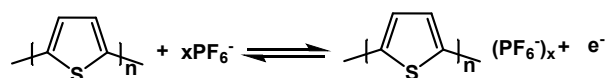
Figure 6. (a) Cyclic performance of SPAN cathodes synthesized at different temperatures; Synthesis process and structure of SPAN (450 °C) is shown in inset. Reproduced with permission.⁵⁹ Copyright 2004, Elsevier. (b) Proposed structure of SPAN, containing all relevant functional groups ($0 < x < 6$; $y = 1, 2$) and (c) its cyclic performance in different electrolytes. Reproduced with permission.⁶⁶ Copyright 2011, American Chemical Society. (d) Schematic illustration of the reaction pathway for SPAN to store lithium. Reproduced with permission.²⁰ Copyright 2018, American Chemical Society. (e) Cycling performance of SPAN cathode with deficient lithium anode at current density of 100 mA g^{-1} in different electrolytes. Reproduced with permission.⁶⁷ Copyright 2019, Elsevier.

Moreover, formation/deformation of an ion-coordination bond between Li^+ and negative location around S/N atoms in SPAN was found to be very fast and reversible, enabling SPAN to deliver the best rate capability and cyclic stability among those reported before. Most of studies mentioned above used carbonate-based electrolyte for electrochemical measurements. However, it is well known that LMA in carbonate-based electrolyte suffers from low coulombic efficiency due to the unstable solid-electrolyte interphase (SEI) formation and dendrite growth. In contrast, LMA in ether-based electrolyte shows higher coulombic efficiency and more uniform lithium deposition. Therefore, Liu's group reported their improved cyclic performance of SPAN cathode using concentrated ether-based electrolyte with LiTFSI and LiNO_3 as co-salts.⁶⁷ SPAN electrode in concentrated electrolyte (4M LiTFSI-DOL-DME) with 0.5 M LiNO_3 showed best cyclic stability and highest coulombic efficiency compared to that in dilute electrolyte (1M LiTFSI-DOL-DME) without LiNO_3 . When deficient LMA was used, SPAN electrode cycled in dilute electrolyte showed rapid capacity drop just within 40 cycles with very low coulombic efficiency as shown in Fig. 6e. These results demonstrated that, polysulfide dissolution happens in a dilute electrolyte and resulting a poor cyclability. In contrast, concentrated electrolyte together with LiNO_3 can not only enable the formation of stable SEI on LMA but also stabilize cathode-electrolyte interphase (CEI) on cathode. Recently, numerous studies were conducted to further improve the cyclic stability of SPAN cathodes in ether-based electrolytes. For example, catalytic amount of Se doping in SPAN (Se_xSPAN , $x < 0.15$, $\sim 50\% \text{Se}_x\text{S}$) resulted in fast Li^+ ion diffusion, relatively low polarization and outstanding compatibility with

ether-based electrolyte.⁶⁸ Composite SPAN cathodes of SPAN-graphene nanosheet (GNS) and SPAN-multi-wall-carbon tube (MWCT) also exhibited improved cyclic stability and rate capability than the bare SPAN due to the electronically conductive network and stable structure created by MWCT and GNS.^{69, 70} Although, these efforts achieved great progress in the improvement of electrochemical properties, more fundamental studies on identifying the molecule structure and understanding the charge storage mechanisms of SPAN cathodes are still needed.

2.3 P-type organosulfide (thioether) cathode materials

Thioether compounds belong to p-type organics, they show different redox behaviors comparing with other organosulfur compounds. Typically, thioethers undergo oxidation first to form stable cationic radical species and further bind with anion from electrolyte such as PF_6^- , ClO_4^- and TFSI^- to remain electroneutral as



Compared with n-type organosulfides, p-type thioether electrodes deliver higher redox potential, which could result in higher energy density. In addition, the redox process of thioether are not accompanied by the cleavage and recombination of the disulfide bonds, therefore kinetics is expected to be faster than disulfide or polysulfide cathodes. It was well accepted that thioether bond could improve the electron transfer due to the π -electron delocalization between the lone pair electrons of sulfur and the aromatic rings.

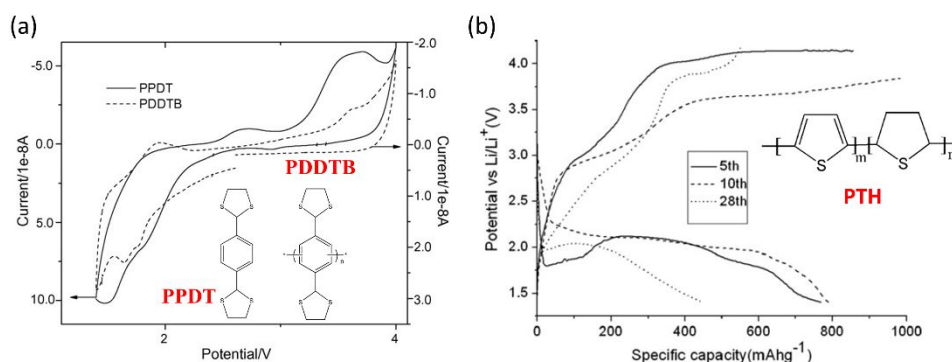


Figure 7. (a) molecular structures of PPDT and PDDTB compounds and their CV curves. Reproduced with permission.⁷¹ Copyright 2007, Elsevier. (b) Molecular structure of PTH polymer and its charge/discharge profiles. Reproduced with permission.⁷⁷ Copyright 2008, Elsevier.

The concept of thioether as cathode in lithium batteries was first introduced by Zhan and coworkers in 2007.⁷¹ They investigated various thioethers either conjugated or unconjugated as cathode materials^{72, 73} and found that these compounds can deliver high capacity of 300-800 mAh g⁻¹ when ether-based electrolytes were used. Fig. 7a shows the molecular structures and CV curves of poly(2-phenyl-1,3-dithiolane) (PPDT) and poly(1,4-di(1,3-dithiolan-2-yl)benzene) (PDDTB) cathodes tested in 1M LiTFSI-DME/DOL (1:2 w/w) electrolyte. The charge behaviors of these two electrodes with such high oxidation peaks are quite different from those of disulfides reported before, indicating that charge storage mechanism might be different. However, electrochemical results show severe fluctuation in cyclic performance for both electrodes. To confirm the thioether bond itself could provide energy storage, their group further designed and synthesized aliphatic thioether polymers and used as electrode for Li battery. Their results indicated that thioethers are electrochemically active and can be used as cathode materials for the rechargeable

batteries.⁷⁴ Polythianthrene, containing two or more benzene rings connected with thioether groups, can be oxidized to its cation state at a voltage ~ 4.1 V versus Li/Li^+ and provide a theoretical capacity of 388 mAh g^{-1} based on four-electron transfer.^{75, 76} Since such high voltage is comparable to the reaction potential of inorganic cathodes, polythiathrene cathode was synthesized and studied as cathode for lithium battery. Unfortunately, it can only provide a specific capacity of 71 mAh g^{-1} , which is much lower than its theoretical value. Thiophene, another p-type organosulfide compound, also has a cyclo-thiolane structure with (C-S-C) configuration was also studied as cathode for lithium battery. Polythiophene (PTH) was prepared by Tang et al.⁷⁷ and tested as cathode for Li battery. In ether-based electrolyte, chemically polymerized PTH exhibited multiple electrochemical oxidation peaks within 3.2-4.4 V and only one broad peak within 1.5-2.0 V, which was slightly different from electrochemically polymerized PTH tested in carbonate-based electrolyte. As shown in Fig. 7b, the maximum capacity of PTH reached as high as 800 mAh g^{-1} but with rapid capacity decay after 20 cycles. These results provided a new direction to utilize thioether compounds as cathode materials with multi-electron reaction for Li battery. However, this type of thioether cathode materials will not be able to make practical significance until their unstable cycling performance and large electrochemical polarization problems can be resolved. More studies are needed to understand the charge storage mechanism of thioether compounds for further optimizing their electrochemical performance.

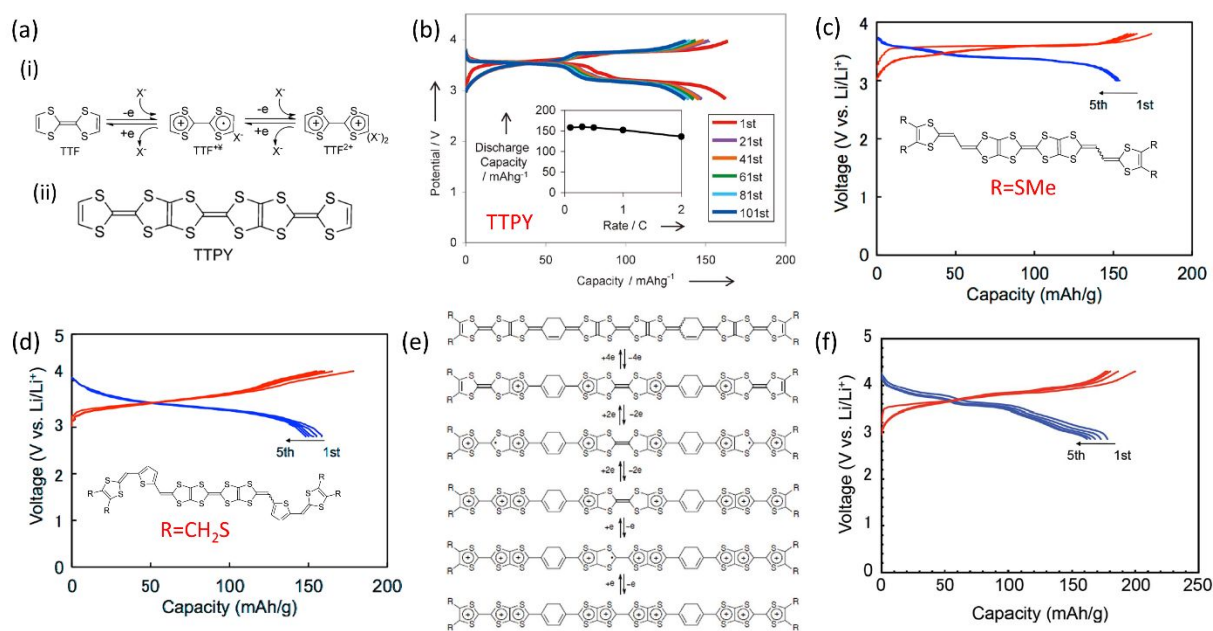


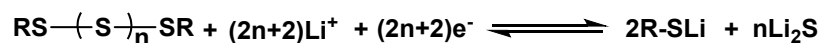
Figure 8. (a) i: Redox process of TTF; ii: molecular structure of TTPY. (b) Galvanostatic charge-discharge curves for TTPY at 0.2 C rate. Inset shows rate performance. Reproduced with permission.⁷⁹ Copyright 2012, Wiley-VCH. (c-d) molecular structure and charge/discharge performances of vinyl extended TTPY with -SMe and -CH₂S groups. Reproduced with permission.⁸⁰ Copyright 2015, Iwamoto et al; licensee Beilstein-Institut. (e) Ten-electron redox process of TTF derivatives and (f) its electrochemical performance. Reproduced with permission.⁸¹ Copyright 2014, Royal Society of Chemistry.

Tetrathiafulvalene (TTF) and its derivatives are also belonging to p-type organosulfur compounds, which exhibit metallic conductivity.⁷⁸ As a typical π -electron donor, TTF has received tremendous attention as high voltage cathode material. As shown in Fig. 8a, TTF exhibits two successive single-electron reversible redox process and forms stable radical cations and di-cations with counter anions that are taken from the electrolyte. The redox potentials of TTF are 3.1 and 3.5 V versus Li/Li^+ in $\text{LiBF}_4/\text{Propylene carbonate}$ (PC) electrolyte system. However, TTF is soluble in the organic electrolyte, hence cannot be used directly as

cathode. Inatomi et al.⁷⁹ introduced TTF 2,2'-bi[5-(1,3-dithiol-2-ylidene)-1,3,4,6-tetrathiapentanylidene] (TTPY), which hardly dissolves in organic solvents. When cycled in the LiBF₄-PC based electrolyte, TTPY delivered initial capacity of 168 mAh g⁻¹ (corresponding to four-electron redox) (Fig. 8b), which was comparable to those of inorganic cathode materials commercially available. Although impressive rate performance of TTPY was exhibited, dissolution of charging products was observed. To solve this, their group synthesized vinyl extended TTPY (V-TTPY) analogs and tris- and pentakis-fused TTF analogues by the insertion of two thiophene rings.⁸⁰ As shown in Fig. 8c-d, V-TTPY analogs with different functional groups exhibited similar charge/discharge behaviors. V-TTPY with -SMe groups delivered five electron redox process with a capacity of 157 mAh g⁻¹, while six electron redox transfer was occurred for V-TTPY with -SCH₂-CH₂-S groups. Both V-TTPY cathodes exhibited relatively stable cyclic performance compared to TTPY cathode. Five stages of redox process with ten electron transfer was achieved from pentakis-fused TTF derivatives extended with two cyclohexene-1,4-diylidenes.⁸¹ This multi-electron cathode delivered a high capacity of 196 mAh g⁻¹ with energy density of 700 Wh Kg⁻¹ (Fig. 8e-f). These results provided rational design strategy to further develop high-energy-density organic electrode materials.

2.4 Organosulfide polymer electrode materials

Organosulfide polymers containing polysulfide bonds formed by copolymerization of melted linear polysulfide and polymerizable linker monomer are confirmed to be able to effectively suppress the long-chain polysulfide dissolution problem in the Li-S batteries due to strong covalent bonds between sulfur and polymer backbone. In organosulfide polymers, the sulfur content can be adjusted by tuning the mass of sulfur chain, while the overall electrochemical performance can be controlled by introducing favorable organic frameworks or functional groups. Organosulfide polymers are containing a chain of sulfur as redox center, in which repeated S-S bonds break and reform during lithiation and delithiation processes to generate lithium thiolates and lithium sulfide as (R is an organic moiety)



Since Wang et al.⁶² firstly designed and synthesized SPAN and successfully applied it as cathode materials for Li-S battery, copolymerization strategies have attracted more and more attention for stabilizing elemental sulfur into polymeric materials. Generally, organosulfide polymers can be obtained by radical insertion reaction of ring opened diradical sulfur with various organic monomers and polymers bearing ether unsaturated hydrocarbons, or Aromatic-H and Aromatic-SH functionalities to form stable C-S bonds.^{82, 83} Synthesizing sulfur-containing polymers directly from molten liquid sulfur in large quantities via inverse vulcanization was firstly reported by Pyun and coworkers in 2013.⁸² Chemically stable poly(sulfur-random-1,3-diisopropenylbenzene) (poly(S-*r*-DIB)) prepared via inverse vulcanization as shown in Fig. 9a, DIB and liquid sulfur was copolymerized at 185 °C to promote efficient ring opening polymerization of S₈. This polymer exhibited very similar charge/discharge behavior to that S₈ with two distinguishable plateaus corresponding to generation of higher order linear polysulfide and further reduced to lower order sulfides down to Li₂S, respectively. Meanwhile, poly(S-*r*-DIB) exhibited high capacity retention and long-term cyclic stability with 823 mAh g⁻¹ capacity at 100 cycle, which was superior compared to S₈ cathode and achieved the highest value among those polymer-based sulfur cathodes reported to date. Lithiation mechanism of this polymer was systematically studied in another work by Pyun and coworkers⁸³ as shown in Fig. 9b. They proposed that, within the high voltage plateau regime, high ordered organosulfur DIB units formed with further reaction generating organosulfur DIB units with shortened oligosulfur and Li₂S₅. At the lower voltage region, fully discharged organosulfur DIB products as well as insoluble mixtures of Li₂S₃ and Li₂S₂ formed. Therefore, the enhanced electrochemical properties of poly(S-*r*-DIB) were originated from these organosulfur units dispersed in insoluble lower order sulfides.

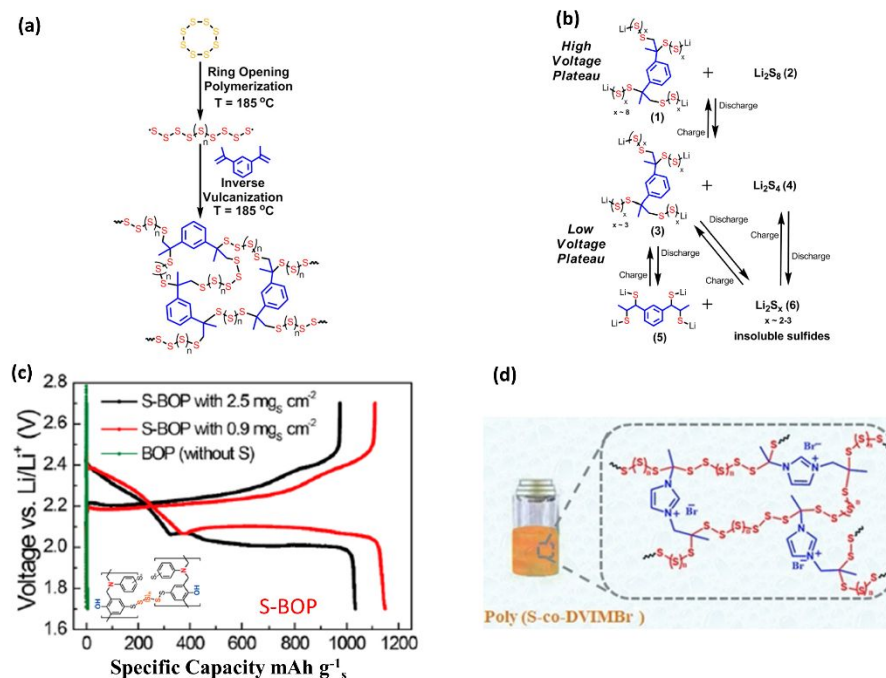
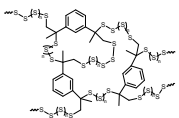
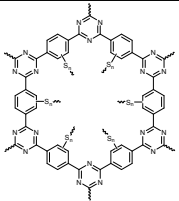
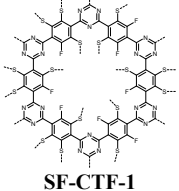
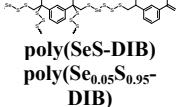
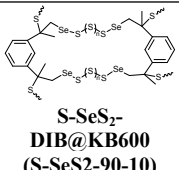
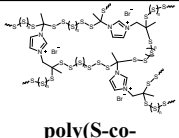


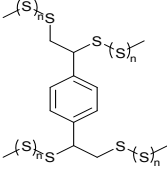
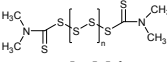
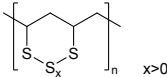
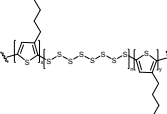
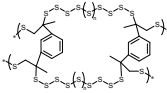
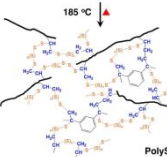
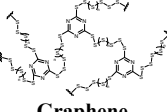
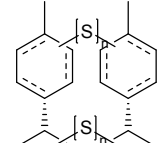
Figure 9. (a) Synthetic scheme for the inverse vulcanization process yielding poly(sulfur-random-1,3-diisopropenylbenzene) copolymers. (b) Possible lithiation mechanism of poly(S-r-DIB). Reproduced with permission.⁸³ Copyright 2014, American Chemical Society. (c) Charge/discharge profiles of S-BOP cathodes with different S loading amount cycled at a current rate of $C/20$. Reproduced with permission.⁸⁶ Copyright 2016, American Chemical Society. (d) Photograph and molecular structure of poly(S-co-DVIMBr). Reproduced with permission.⁸⁸ Copyright 2020, Wiley-VCH.

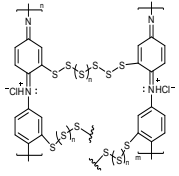
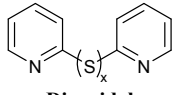
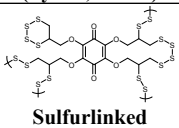
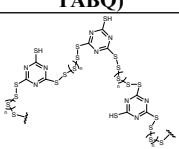
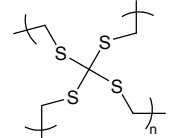
Coskun's group⁸⁴ reported synthesis of sulfurized covalent triazine framework (S-CTF) from 1,4-dicyanobenzene and elemental sulfur without any catalysts or solvents. In this polymer, S was bonded to CTF through C-S and content of sulfur reached up to 62 wt%. Later, their group⁸⁵ employed nucleophilic aromatic substitution reaction ($\text{S}_\text{N}\text{Ar}$) between perfluoroaryl units and elemental sulfur to synthesize fully conjugated organosulfur polymer with 86% of Sulfur content, which is much higher than that previously reported carbon/S composites. Their approach not only enabled homogeneously distribution of sulfur within large π -conjugated framework but also effectively mitigated the polysulfide shuttling. As a result, sulfur utilization and kinetics of Li-S system were improved significantly. Choi et al.⁸⁶ reported orthogonal synthetic approach to prepare sulfur-embedded polybenzoxazine (S-BOP) with a sulfur loading of ~ 72 wt%. In their approach, to increase the sulfur loading amount, the elemental sulfur was chemically impregnated with thiol functionalized benzoxazine monomer. S-BOP cathode demonstrated an unusual discharge profile with slope in the range of 2.4–2.05 V as shown in Fig. 9c, which is slightly different from the typical discharge curve of elemental sulfur showing two clear plateaus at 2.1 and 2.4 V. The initial reversible capacity of S-BOP cathode was about 1110 mAh g^{-1} with a high coulombic efficiency of 96.6%, indicating that polysulfide shuttling is successfully suppressed. S-BOP cathode also delivered excellent cyclic performance as 92.7% of initial capacity was achieved after 1000 cycles at a high current rate of 1C. These approaches provided valuable direction of utilizing sulfur as cathode for high performance Li-S batteries. More recently, various methods have been reported to further optimize the long-term cyclic stability and rate performances of organosulfur polymers. One of the effective approaches is taking the advantages of the chemical similarity of selenium (Se) with sulfur, but higher electronic conductivity. Application of hybrid chalcogenide polymer of S and Se in Li-S system was firstly reported by Gomez et al.⁸⁷ By following

the research on poly(S-r-DIB), they prepared various poly (Sulfur-*r*-Selenium-*r*-DIB) (poly(S-*r*-Se-DIB) compounds with different Se :S ratio via similar inverse vulcanization reaction. Among those co-polymers, the (poly(S-*r*-Se-DIB) with 5 % and 7.5 % Se in mol exhibited high capacity retention and rate capability compared with that of others as well as poly(S-r-DIB). They suggested that higher conductivity of the Se facilitated the electron transportation through the active materials and further improved the kinetics. In addition, the high electroactivity of low order Li₂Se increased the reversible capacity and reduced the active material loss, therefore rendering excellent cyclic performance. A novel sulfur-rich polymer cathode containing ionic liquid segments named poly(sulfur-co-1-vinyl-3-allylimidazolium bromide) (poly(S-co-DVIMBr)) was also prepared via inverse vulcanization of S₈ with DVIMBr as ionic liquid linker for the first time.⁸⁸ In this structure (Fig. 9d), presence of imidazolium N⁺ cations were expected to serve as chemical adsorption site for immobilizing polysulfides, while introduction of ionic liquid groups was expected to improve the ionic conductivity. Results demonstrated that lithium diffusion kinetics of poly(S-co-DVIMBr) was improved by nearly 10 times during redox reactions, compared with the copolymer without ionic liquid segment. Moreover, 90.22 % of capacity retention was obtained for this polymer even after 900 cycles. These results provided new strategy of introducing functional group with cations into organosulfide polymers for optimizing the electrochemical performance. Structure and electrochemical performances of other representative organosulfur polymer cathodes were summarized in the Table 3.

Table 3. Molecular structures and electrochemical performances of recently reported organosulfide polymers.

Materials	Specific Capacity (mAh g ⁻¹)/ Current density (mA g ⁻¹) or C rate	Capacity retention (mAh g ⁻¹)/cycle number/ current density (mA g ⁻¹)	Rate performance Specific Capacity (mAh g ⁻¹)/ Current density (mA g ⁻¹)	Sulfur content	References Notes
 poly(sulfurrandom-1,3-diisopropenylbenzene) (poly(S-r-DIB))	1100(1 st)/167.2 (1.7-2.6V)	823/100/167.2	~400/3344 (2C)	90 wt%	⁸² 0.38 M LiTFSI and 0.32M LiNO ₃ -DOL/DME (1:1, v/v)
	1225(1 st)/167.2 (1.7-2.6V)	1005/100/167.2 817/300/167.2 635/500/167.2	~360/3344 (2C)	90 wt%	⁸³ 0.38 M LiTFSI and 0.32M LiNO ₃ -DOL/DME (1:1, v/v)
 Covalent triazine frameworks S-CTF-1	670(1 st)/25 (1.7-2.7V)	414/300/500 329/300/1000	406.3/1000 (2C)	62 wt%	⁸⁴ 1M LiTFSI - TEGDME/DIOX (0.33:0.67, v/v) + 0.2M LiNO ₃
 SF-CTF-1	1138.2(1 st)/50 (1.8-2.7V)	520.1/300/1000 435.1/300/2000 330.3/300/5000	374/5000 (5C)	86 wt%	⁸⁵ 1M LiTFSI - TEGDME/DIOX (0.33:0.67, v/v) + 0.2M LiNO ₃
	1296(1 st)/167.5 (1.7-2.8V)	833/150/837.5	~600/1675 (1C)	~51 wt%	⁸⁹ 1M LiTFSI-DOL/DME (1:1, v/v) + 0.5 wt% LiNO ₃
 Sulfur-embedded polybenzoxazine (S-BOP)	1034(1 st)/31 (1.7-2.7V)	584.01/1000/720	~550/1440 (2C)	72 wt%	⁸⁶ 1M LiTFSI-TEGDME/DIOX (0.33:0.67, v/v) + 0.2M LiNO ₃
 poly(SeS-DIB) poly(Se_{0.05}S_{0.95}-DIB)	860/324.4 (1.7-2.6V)	~700/100/648.8	550/1622 (1C)	S + Se: 90 wt%	⁸⁷ 0.38 M LiTFSI and 0.32M LiNO ₃ -DOL/DME (1:1, v/v)
 S-SeS₂-DIB@KB600 (S-SeS₂-90-10)	1218(1 st)/100 (1.8-2.8V)	~600/500/1000	585/2000	S + Se: 90 wt%	⁹⁰ 1M LiTFSI-DOL/DME (1:1, v/v) + 0.2M LiNO ₃
 poly(S-co-DVIMBr)	1161(1 st)/167 (1.7-2.8V)	638/150/1670 517/900/3340	573/3340 (2C)	65.49 wt%	⁸⁸ 1M LiTFSI-DOL/DME (1:1, v/v) +0.2M LiNO ₃

 <p>(p(S-DVB)) (80:20)</p>	1100(1 st)/0.1C (1.6-2.8V)	650/50/0.1C	200/0.5C	79.8%	⁹¹ LiFSI/PEO and LiTFSI/PEO dry solid electrolytes
 <p>tetramethylthiuram disulfide-sulfur (TMTD-S)</p>	TMTD-S: 685(1 st)/212.2 TMTD-S with Ketjen Black: 1054(1 st)/212.2 (1.5-2.8V)	TMTD-S: 540/200/212.2 TMTD-S with Ketjen Black: 930/100/530.5	TMTD-S: ~250/8488 (8C)	50 wt%	⁹² 1M LiTFSI- DOL/DME (1:1,v/v)+ 0.1M LiNO₃
 <p>Organic polysulfane nanosheets (OPNS)</p>	891(1 st)/1670 (1.7-2.7V)	811/620/1670	562/16700 (10C)	72 wt%	⁹³ 1 M LiTFSI and 0.1 M LiNO₃- DOL/DME (1:1 v/v)
 <p>copolymer CP(S3BT)</p>	1362(1 st)/0.1C (1.5-3.0V)	682/500/1C	631/(5C)	70 wt%	⁹⁴ 1M LiTFSI- DOL/DME (1:1, v/v) + 0.1M LiNO₃
 <p>Carbon/polymeric sulfur (C/PS) composites</p>	1105(1 st)/0.5C (1.7-3.0V)	889/100/0.5C	681/ (5C)	70 wt%	⁹⁵ 1M LiTFSI- DOL/DME (1:1, v/v) + 0.1M LiNO₃
 <p>Covalently grafted polysulfur- graphene nanocomposite (polySGN)</p>	1135(1 st)/0.05C (1.7-2.8V)	760/100/0.05C 717/100/0.1C 642/100/0.2C	~800/ (0.2C)	~70 wt%	⁹⁶ 1.85M LiTFSI- DOL/DME (1:1, v/v) +0.1M LiNO₃
 <p>Graphene- supported crosslinked sulfur copolymer nanoparticles, cp(S- TTCA)@rGO-80</p>	1341 (1 st)/0.1C (1.5-3.0V)	671/500/1C	645/ (5C)	81.79 wt%	⁹⁷ 1M LiTFSI- DOL/DME (1:1, v/v) + 0.1M LiNO₃
 <p>Sulfur-limonene polysulfide (LSP) Carbin black-LSP</p>	~1000(1 st)/0.5C (1.6-2.8V)	932/300/0.5C	510/ (5C)	59%	⁹⁸ 0.5M LiTFSI- DOL/DME (1:1,v/v) +1 wt% LiNO₃

 <p>Copolymer cp(S-PMAT)</p>	1240 (1 st)/167.2 (1.5-3.0V)	495/1000/3344	600/8360 (5C)	61 wt%	⁹⁹ 1M LiTFSI-DOL/DME (1:1 v/v) +0.1M LiNO ₃
 <p>Dipyridyl polysulfides (Py2S_x, 3 ≤ x ≤ 8)</p>	391.7(1 st)/425.4 (2.0-3.0V)	273.8/1200/425.4	273.7/2127 (5C)	N/A Theoretical capacity (425.4 mAh g ⁻¹)	¹⁰⁰ 1M LiTFSI-DOL/DME (1:1 v/v) + 0.15M LiNO ₃
 <p>Sulfurlinked tetra(allyloxy)-1,4-benzoquinone (S-TABQ)</p>	1346(1 st)/167 1077(1 st)/1670 (1.7-2.7V)	722/500/1670 911/400/167	833/16700 (10C)	75 wt%	¹⁰¹ 1M LiTFSI-DOL/DME (1:1 v/v) +0.1M LiNO ₃
 <p>TTCA</p>	1210(1 st)/167.5 (1.7-2.7V)	872/300/335 886/300/837.5	730/8375 (5C)	63 wt%	¹⁰² 1M LiTFSI-TEGDME/DIOX (0.33:0.67, v/v) +0.2M LiNO ₃
 <p>poly[methanetetrayl tetra(thiomethylene)] (PMTTM)</p>	504(3 rd)/50 (1.4-4.2V)	200/10/50 ~110/50/50	N/A	N/A Theoretical capacity (570 mAh g ⁻¹)	⁷⁴ 1M LiTFSI-DOL/DME (2:1 wt%)

3. Application of organosulfur compounds as lithium battery components other than cathode: binder, additive, and artificial SEI layer

As summarized above in Table 2-3, organosulfur compounds are promising cathode materials for next generation rechargeable battery systems. In addition to their application as electrode for Li battery, organosulfur compounds also have been investigated as electrolyte additive in helping the formation of stable cathode/electrolyte or anode/electrolyte interphases (CEI/SEI). Several studies also demonstrated that organosulfur polymers can be utilized as artificial SEI layer on LMAs, as well as binder for Sulfur cathode.

3.1 Organosulfur compounds used as electrolyte additive for Li-S or Li-O₂ batteries

As mentioned in the previous section, long order lithium polysulfides are generated at the beginning of the discharge in Li-S cell. These polysulfides are soluble in electrolyte and highly reactive with LMA after migrating to LMA surface, resulting in formation of insoluble lithium sulfides and disulfides (Li₂S and Li₂S₂) at the anode. As a result, Li-S cell shows poor cycling life due to the decreasing of active S in the battery as well as formation of nonuniform SEI on LMA. To solve this problem, Trofimov et al.¹⁰³ synthesized a series of protected bis(hydroxyorganyl) polysulfides (BHPS) and used them as additives to enhance the solubility of low-order Li₂S_m (1 ≤ m ≤ 2) precipitated on LMA surface. They proposed that

BHPS can react with lithium sulfides and disulfides and move back to the cathode surface to participate in electrochemical reaction with regeneration of soluble polysulfide molecules. Their result showed that Li-S cell exhibited much higher capacity and longer cyclic performance by adding tri(methyl)silyl substituted BHPS in the electrolyte. DMDS (CH_3SSCH_3) is one of the small-molecule organodisulfide cathode materials containing a S-S bond that can reversibly cleave and reform during electrochemical reaction. However, DMDS was not successfully utilized as cathode due to its high solubility in the electrolyte. Wang's²¹ group attempted to use DMDS as co-solvent to replace inactive part of electrolyte solvent to achieve higher energy density. As shown in Fig. 10a, the high voltage discharge plateau for S cathode disappeared with DMDS contained electrolyte, which is much obvious when the DMDS concentration was increased. More importantly, the initial discharge capacity of Li-S cells increased with increasing DMDS content in electrolyte and highest capacity of 1950 mAh g^{-1} was achieved for electrolyte containing 50% of DMDS. The capacity retention and rate performances were also improved by introducing DMDS as co-solvent. They found that Li-S cell with DMDS has a new reduction pathway due to the formation of soluble methyl-terminated polysulfide (DMPS) intermediates which can be further reduced to lithium organosulfides. Therefore, DMDS-containing electrolyte can not only provide extra capacity but also enable robust performance of S cathode. In their latest report¹⁰⁴, they investigated the role of DMDS in Li-S system with different electrolyte/sulfur (E/S) and carbon/sulfur (C/S) ratios to figure out whether it can be used in lean electrolyte condition or not. The proposed reaction mechanism of Li-S cells with low and high C/S ratios in DMDS containing electrolyte are shown in Fig. 10b (i, ii, and iii). It demonstrated that S cathode with high C/S ratios enables reduction of more amounts of lithium organosulfides to CH_3SLi and Li_2S due to the more conductive surface provided by carbon for the interfacial reactions of DMPS intermediates, which would contribute to higher sulfur specific capacity (2500 mAh g^{-1}). Decreasing E/S ratio is of critical importance to practical cell energy density, but it is very challenging to decrease E/S ratio in Li-S system. DMDS-containing electrolyte was able to enable cell to maintain good cycling performance even with a low E/S ratio of 5 compared to DMDS-free electrolyte with a same E/S ratio. Later, Dimethyl trisulfide (DMTS) was also studied as electrolyte additive for Li-S cell for increasing the specific capacity.^{105, 106} Taking advantage of DMTS, which has higher reactivity and could provide higher capacity with -S-S-S- bonds cleavage, 25 vol% DMTS-containing electrolyte enabled Li-S cell to deliver higher discharge capacity and better capacity retention than the electrolyte using DMDS as co-solvent. These studies provided an effective approach for improving the practical energy density and cyclic performance of Li-S cells. However, agglomeration of Li_2S on cathode side could cause capacity decay, while DMDS and its products migrate to anode side leading to the degradation of LMA. P-type organosulfur compound also showed promising application in Li- O_2 battery, which is another high energy battery system but suffering large overpotential due to the sluggish kinetics of electrochemical reaction. The main discharge product Li_2O_2 generally required higher decomposition energy, leading to high overpotential and side reactions. To overcome this challenge, Zhang et al.¹⁰⁷ utilized TTF as redox mediator to promote decomposition of Li_2O_2 . When coupled with LiCl as additive in the electrolyte, organic conductor $\text{TTF}^+\text{Cl}_x^-$ precipitate covered on Li_2O_2 to provide an additional electron-transfer pathway, which significantly reduced the over-potential and improved the efficiency of Li- O_2 cell.

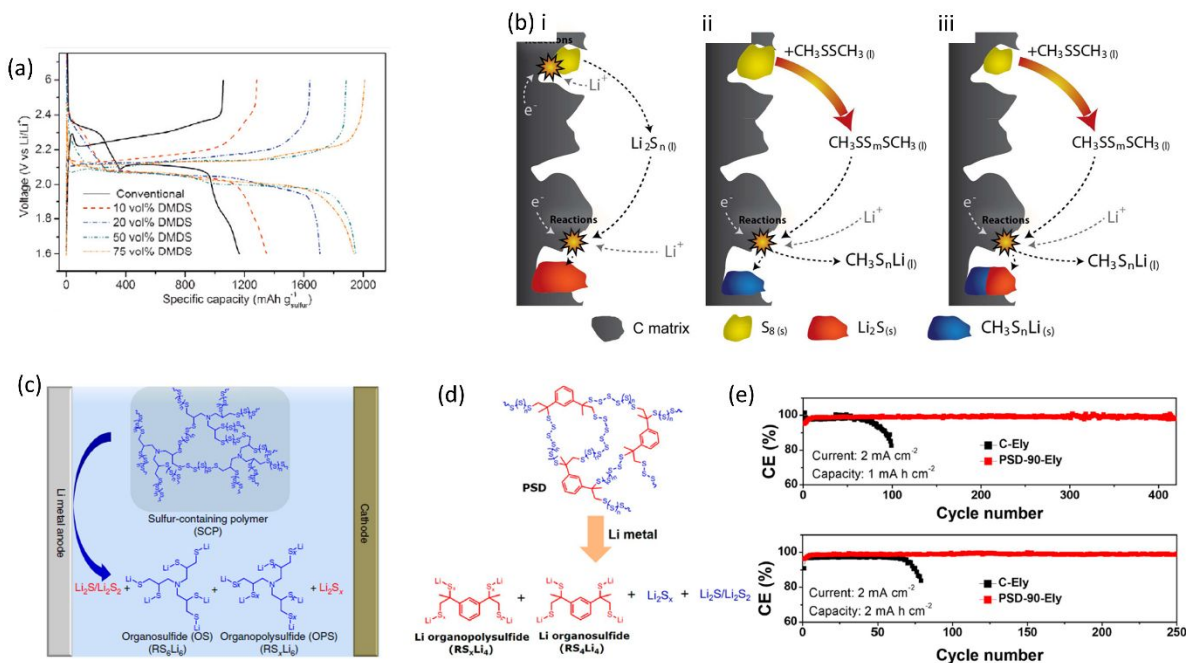


Figure 10. (a) Initial discharge-charge profiles of C/S cathodes at C/10 rate in conventional and 10-75 vol% DMDS-containing electrolytes. Reproduced with permission.²¹ Copyright 2016, Wiley-VCH. (b) Schematic diagrams of the discharge mechanism of surface species at the surface of carbon materials in (i) conventional ether-based Li-S electrolytes and (ii, iii) DMDS-containing electrolytes with tuned low (ii) and high (iii) C/S ratios in the cathodes, showing the shutoff of the discharge process due to electrode surface passivation by different solid precipitates. Reproduced with permission.¹⁰⁴ Copyright 2017, Elsevier. Schematic illustration of the formation of stable inorganic/organic hybrid SEI layer on LMA from (c) PST, Reproduced with permission.¹⁰⁸ Copyright 2017, Nature Publishing Group. (d) PSD additives. (e) Coulombic efficiencies of Li-Cu cells at 2 mA cm⁻² with different capacities. PSD-90: sulfur content is 90% in PSD polymer. C-Ely: 1M LiTFSI-DOL/DME (1/1 v/v) with 1 wt% LiNO₃. Reproduced with permission.¹⁰⁹ Copyright 2018, American Chemical Society.

3.2 Organosulfur compounds used as electrolyte additive or artificial SEI layer for Li metal anode protection

LMAs with a high theoretical capacity of 3860 mAh g⁻¹ and low electrochemical potential of -3.045 V (vs. standard hydrogen electrode) has been considered as a promising anode candidate for next-generation rechargeable battery. However, practical application of LMA has been hindered by low coulombic efficiency (CE) and safety concerns caused by dendrite formation. One of the critical issues is the formation of unstable SEI layer on LMA surface, leading to uneven lithium deposition as well as electrolyte consumption. Over the years, strategies have been implemented to modify LMA surface by optimizing electrolyte components, using SEI film forming additives as well as forming artificial SEI. Wang's group successfully pioneered the use of organosulfide/organopolysulfides as "plasticizer" in the SEI layer to improve the mechanical flexibility and stability.¹⁰⁸ They synthesized poly(sulfur-random-triallylamine) (PST) through a direct copolymerization of S₈ and vinylic monomer triallylamine and used as electrolyte additive in Li-S battery. It was proposed that, PSTs can be electrochemically decomposed into Li organosulfides (RS₆Li₆), Li organopolysulfides (RS_xLi₆), Li₂S_x, and Li₂S/Li₂S₂ by contacting Li metal as

shown in Fig. 10c. During Li deposition/stripping, such a flexible organic/inorganic hybrid SEI layer could be self-formed on the top of deposited Li, hence protect LMA and improve its electrochemical performance. As expected, much more uniform and compact lithium deposition was observed with a higher average CE of 99% over 400 cycles in Li/Cu cell at relatively higher current rate. Meanwhile, Li-S cell cycled in the PST containing electrolyte also showed long cycling life over 1000 cycles and good capacity retention. These results demonstrated that organosulfur compounds with modified molecular structure can enable the formation of flexible and more stable SEI on LMA surface. This group also developed an aromatic-based sulfur-containing polymer poly(sulfur-random-1,3-diisopropenylbenzene) (PSD) as a good SEI forming additive for LMA.¹⁰⁹ Similar as the previous result, this polymer can be chemically/electrochemically decomposed to self-form a flexible SEI containing organopolysulfides and inorganic sulfur species on LMA. The uniqueness of PSD compared to PST is the π -conjugated planner backbone of aromatic organic components can facilitate the flat morphology of SEI and improve its toughness and flexibility (Fig. 10d). Therefore, dendrite free lithium deposition/stripping with a higher average CE of 99.1% with longer cycling life were achieved with PSD additive especially with higher sulfur content (90%), which is better than that of Li-Cu cell cycled in linear PST containing electrolyte (Fig. 10e). In addition to the electrolyte additives, research on artificial SEI layer either organic, inorganic or hybrid has been attracting more attentions for the realization of safe and highly stable LMAs.¹¹⁰ More recently, successful utilization of organosulfur polymers as artificial SEI on LMA was demonstrated by Zhao et al.¹¹¹ In their work, a multifunctional sulfur containing polymer (MSCP) was chemically cross-linked on LMA surface *in situ*, which was the incorporation of lithium polysulfidophosphate components in the inorganic sulfur containing group. After chemically cross-linking, Li_3PS_x was formed along with organopolysulfides and inorganic lithium sulfides. Among this inorganic/organic hybrid SEI, Li_3PS_x facilitated the Li ion transport through the SEI layer due to its higher Li ion conductivity, while organopolysulfides enabled SEI become more resilient to accommodate the volume fluctuation of LMA during cycling. When the MSCP protected LMA paired with LiFePO_4 cathode, it exhibited significantly increased coulombic efficiency and better long-term cyclic performance with a capacity retention of ~89.4% even after 500 cycles which is much better than the bare LMA. More importantly, such a MSCP layer can be produced for large scale, which could promote practical application of LMA. Separator architecture design, for example, coating inorganic and organic compounds on the surface of the separator, is another important strategy to stabilize LMA performance since the electrolyte wettability, mechanical strength and thermal conductivity of separator can be optimized by surface coating.¹¹² W. He and coworkers reported a facile and cost-effective approach to make Li deposition more uniform by doping the separator with garlic ingredients¹¹³, which contains rich organosulfur compounds such as allicin ($\text{C}_6\text{H}_{10}\text{OS}_2$), alliin/isoalliin ($\text{C}_6\text{H}_{11}\text{NO}_3\text{S}$), diallyl disulfide ($\text{C}_6\text{H}_{10}\text{S}_2$), and S-allyl cysteine ($\text{C}_6\text{H}_{11}\text{NO}_2\text{S}$). These components participated in the SEI formation and covered grain boundaries of the inorganic components in SEI, thus the flexibility was improved significantly. These proof-of-concept studies in utilization of organosulfur polymers can inspire new strategies for the development of inorganic/organic hybrid SEI layer for LMAs.

3.3 Organosulfur compounds used as CEI forming additive for high voltage inorganic cathode materials

Layered transition metal oxides such as LiCoO_2 and $\text{LiNi}_x\text{Co}_y\text{Mn}_{1-x-y}\text{O}_2$ (NMC) are widely used as cathode materials for commercialized LIBs. One major target for the next-generation LIBs is to reach higher operation voltage to further increase the energy density of these cathodes. However, high voltage operation leads to fast capacity decay and low CE in conventional electrolyte due to the aggressive oxidation of the electrolyte. Even within the commonly considered stable working potential window of the electrolyte (for ex. ~4.3 V for carbonate-based electrolyte), the side reactions between electrolyte and highly reactive charged cathode are hardly avoidable, resulting in thicker unstable CEI formation and severe capacity decay.

It is well accepted that, formation of stable CEI layer from electrolyte additives or modification of cathode surface by doping/coating inorganic or organic components are efficient and economical ways to suppress such side reactions. P-type organosulfur compounds have a high oxidation potential over 4.0 V vs. Li^+/Li and are expected to polymerize electrochemically on cathode surface during charging. Thiophene (TH) and its derivatives were investigated as a stable CEI forming additive for LiCoO_2 and NMC cathodes.

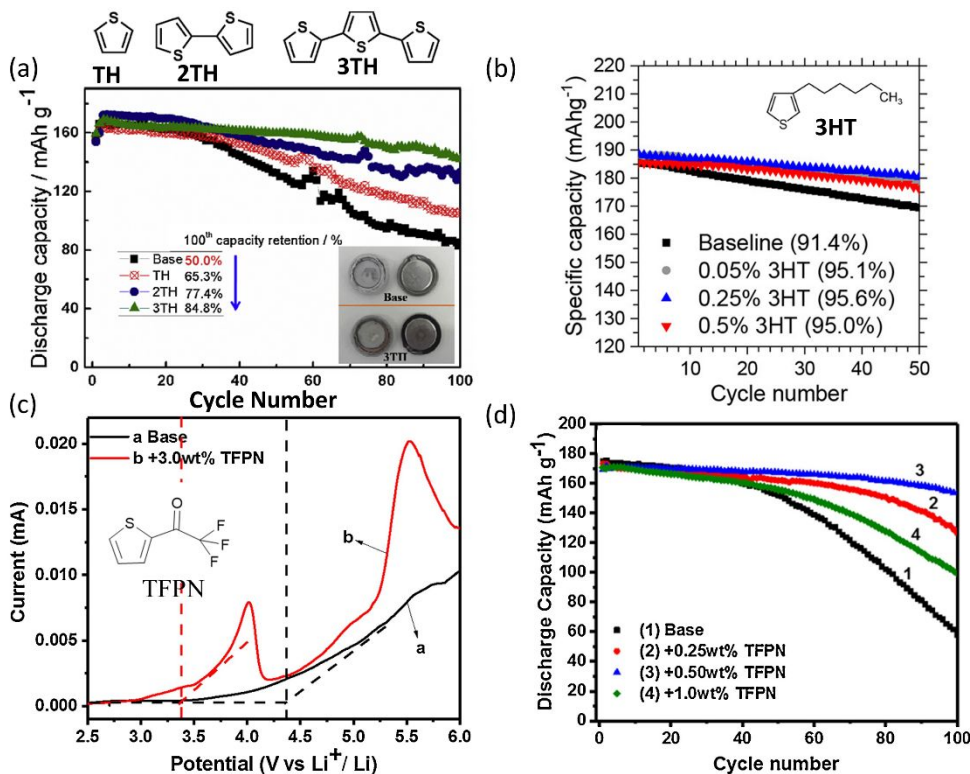


Figure 11. (a) Cycle performances of Li/LiCoO_2 cells in 1 M $\text{LiPF}_6/\text{EC} + \text{DMC}$ (3/7, v/v) and with 0.1 wt% of TH, 2TH, 3TH additives at current density of 0.25 C within voltage range of 3.0-4.4 V. Reproduced with permission.¹¹⁵ Copyright 2015, Elsevier. (b) The cycling performance of $\text{Li}/\text{NMC622}$ cell with different concentration of 3HT additive.¹¹⁷ Copyright 2017, American Chemical Society (c) Linear sweep voltammograms of 1 M $\text{LiPF}_6/\text{EC} + \text{DEC}$ (1/1, v/v) solutions with: a. no additive and b. 3.0 wt% TFPN in stainless steel||Li metal cell (scan rate is 0.2 mV s^{-1}). (d) cyclic performances of Li/LiCoO_2 coin cells with 1 M $\text{LiPF}_6/\text{EC} + \text{DEC}$ (1/1, v/v) solutions without and with TFPN additive of 0.25 wt%, 0.50 wt%, 1.0 wt%, cut-off voltage of 3.0-4.4 V, initial 3 cycles at 0.1 C for activation, then cycle at 0.5 C. Reproduced with permission.¹¹⁹ Copyright 2020, Elsevier.

In 2009, Kim et al.¹¹⁴ attempted to improve the high voltage performance and thermal stability of LiCoO_2 cathode by introducing thiophene (TH) as additive in the electrolyte. The results demonstrated that the oxidation decomposition of electrolyte at high voltage (charge to 4.4 V) was suppressed by adding a little amount of TH, which was further supported by much improved cyclic stability and lowered overpotential. However, oxidation potential of TH is about 4.42 V vs. Li^+/Li , which might be little too high to form enough conductive film on the cathode surface when cell only charged to 4.4 V. Therefore, oligomers of thiophene including 2,2'-Bithiophene (2TH), and 2,2':5',2''-Terthiophene (3TH) were introduced as electrolyte additives for LiCoO_2 cathode.¹¹⁵ Based on the theoretical calculation and experimental results, the oxidation potential decreases gradually with increasing number of TH unit in the molecule (3.95 V for 2TH and 3.8 V for 3TH). Cyclic performances of LiCoO_2 cathode within voltage range of 3.0-4.4 V is shown in Fig. 11a

with TH, 2TH and 3TH as additives. Results demonstrated that LiCoO₂ cathode cycled in 0.1 wt% of 3TH containing electrolyte delivered highest capacity retention of 84.8 % after 100 cycles than that of cycled in baseline electrolyte and electrolyte with TH, 2TH additives. Amine and coworkers reported the positive effect of 3-Hexylthiophene (3HT) with a high oxidation potential of 4.3 V as electrolyte additive, which formed conductive (conductivity range from 10 to 10³ S cm⁻¹) and conjugated polymer during charging, resulting in significant increase in cyclic stability of Li-rich Li_{1.2}Ni_{0.15}Co_{0.1}Mn_{0.55}O₂, and high voltage LiNi_{0.5}Mn_{1.5}O₄ cathodes, especially for the cell cycled at 55 °C.¹¹⁶ They also systematically investigated the additive effects and mechanism of 3HT for LiNi_{0.6}Mn_{0.2}Co_{0.2}O₂ (NMC 622) cathode when higher cut off voltages for charging were applied (Fig. 11b). They proposed that 3HT not only enables formation of robust CEI on cathode but also serves as a “corrosion inhibitor film” against protons (H⁺) formed by electrolyte oxidation.¹¹⁷ These results provided valuable information for the future development of high-voltage electrolyte additives. In addition to the electrolyte additive, thiophene derivatives were coated on cathode surface to form protective layer. Xu et al.¹¹⁸ successfully built an ultra-conformal, highly electronically conductive and ionically permeable poly(3,4-ethylenedioxythiophene) (PEDOT) skin on LiNi_{0.33}Mn_{0.33}Co_{0.33}O₂ (NMC111), Ni-rich LiNi_{0.85}Co_{0.1}Mn_{0.05}O₂ and Li-rich Li_{1.2}Mn_{0.54}Ni_{0.13}Co_{0.13}O₂ cathodes. Multi-model advance characterization techniques were also utilized for investigating the critical role of PEDOT skin. Electrochemical testing and differential scanning calorimetry (DSC)-thermogravimetric analysis results demonstrated that PEDOT coating layer significantly improves capacity retention and thermal stability of both Ni-rich LiNi_{0.85}Co_{0.1}Mn_{0.05}O₂ and Li-rich Li_{1.2}Mn_{0.54}Ni_{0.13}Co_{0.13}O₂ cathodes. Based on the characterization results, it was found that PEDOT skin can mitigate the formation of intragranular cracking within primary particles even after long-term cycles by suppressing the oxygen release from the cathode. NMC111 cathode with PEDOT skin also showed stable impedance due to the improvement of CEI layer and maintaining the ionic and electronic conductivity of the interface. Moreover, the dioxane ring in the molecular structure of PEDOT can chemically coordinate with HF produced by the decomposition of the electrolyte through formation of O-H-F covalent bond, suppressing the transition metal cation dissolution. More recently, Yu's group¹¹⁹ firstly introduced 2-(trifluoroacetyl) thiophene (TFPN) as film-forming additive for enhancing the CEI stability of LiCoO₂ cathode, especially for high voltage operation. Linear sweep voltammograms results (Fig. 11c) show that the oxidation voltage of TFPN additive is about 3.4 V, indicating that TFPN can be oxidized before the decomposition of the electrolyte. In addition to the highly conductive and chemically stable CEI layer formed by electrochemically polymerization of TFPN additive, the perfluorinated alkyl (-CF₃) group in this compound can improve the wettability of the electrolyte toward the separator due to the higher affinity between the nonpolar -CF₃ group and separators. As expected, the LiCoO₂ cathode cycled in the electrolyte with 0.5% of TFPN additive demonstrated much improved cyclic stability with a capacity retention of 90% after 100 cycles as shown in Fig. 11d. in contrast, the LiCoO₂ cathode cycled in the baseline electrolyte only delivered a capacity retention of 33% after 100 cycles. Although there are only limited reports about organosulfur compounds used as CEI protective additive for high-voltage cathodes, the results summarized above clearly demonstrated the potential of organosulfur compounds in protecting the surface of high-voltage cathodes.

3.4 Organosulfur compounds used as binder or additive for Sulfur cathode

Utilization of functionalized binder for sulfur cathode is also quite important for controlling the polysulfide dissolution as well as buffering the volume expansion caused by cycling of sulfur cathode. Polyvinylidene fluoride (PVDF) and polyethylene glycol (PEO) are commonly used in sulfur cathode. However, they are not able to suppress the volume expansion of sulfur cathode and prevent the shuttling of polysulfides, especially for high sulfur loading cathodes. PEDOT: PSS (poly(styrenesulfonate)) based conductive polymers were successfully introduced as binder or coating layer to improve the electrochemical performance of sulfur cathode due to their high electronic conductivity (up to 4600 S cm⁻¹). Cui et al.¹²⁰

investigated the role of PEDOT polymer on sulfur cathode using Ab initio simulations. They proposed that not only the physical confinement of lithium polysulfides within the conductive polymer shells but also the chemical bonding between the heteroatoms in PEDOT with lithium sulfides played essential role for improving the cyclic stability. Inspired by this result, Zhang et al.¹²¹ used polyacrylic acid (PAA) and PEDOT: PSS (poly(styrenesulfonate)) as a binder for sulfur cathode. By taking the advantages of swelling property of PAA with good electronic conductivity and the chemical/physical absorption ability of PEDOT: PSS with lithium polysulfide and lithium sulfides, PAA/PEDOT: PSS binder enabled the Li-S battery exhibits higher initial capacity and stable long-term cyclability. Wei et al.¹²² designed and prepared flexible and binder-free electrode by combining the PEDOT-encapsulated diamond shape sulfur with single-walled carbon nanotubes (SWCNTs). Such a free-standing sulfur cathode presented higher electronic conductivity and remarkable electrochemical performance than that of the elemental sulfur. More recently, a cross-linked PEDOT-PSS polymer with 3-D structure was prepared using divalent Mg^{2+} ion as a cross-linker.¹²³ High electrical conductivity and robust 3-D network structure of PEDOT-PSS- Mg^{2+} binder significantly improved the capacity retention and rate performance of sulfur cathode compared with the PVDF binder. More importantly, water was used for cathode slurry preparation with PEDOT-PSS- Mg^{2+} binder rather than any organic solvents, making the fabrication of Li-S batteries more environmentally friendly. In addition to the PEDOT based polymers, a comb-like ion-conductive organo-polysulfide polymer (PSPEG) binder was prepared by Yang and coworkers to solve the polysulfide shuttling problem.¹²⁴ PSPEG is containing a mass of organo-polysulfide ($-S_x-$) in the main chain and low-molecular-weight PEG on the side chain. They found that $-S_x-$ bonds in the main chain not only improves the compatibility of binder with active material, but also acts as mediator to improve the kinetics of electrochemical reaction and then to promote the redistribution and deposition of the agglomerated S/Li₂S. At the same time, PEG on the side chain provided more Li⁺ transport paths to improve the rate performances of S cathode. As a result, the sulfur cathode with PSPEG binder delivered improved cycling performance and rate capability with a high capacity retention of 91.9 % after 500 cycles at 0.5 C. These studies demonstrated that molecularly designed organosulfur polymers can be used as multi-functional binder for S cathode to improve the sulfur utilization and sluggish kinetics of Li-S batteries.

4. Conclusion and prospective

In summary, this review provides an overview of different types of organosulfur electrode materials and structure related electrochemical performance as well as effective strategies for optimizing the cyclic stability of them. The important role of organosulfur compounds as cathode/anode film forming additive, redox mediator for Li-O₂ and Li-S batteries as well as binder for sulfur cathode are also covered. Although tremendous efforts have been made to enhance the electrochemical performance of organosulfur electrodes, there are still several barriers need to be overcome before the large scale applications of organosulfur electrode materials can be realized. First, electrochemical performance of these electrode materials has not been systematically investigated. Fast charge capability, capability to work under lean electrolyte condition (low electrolyte/sulfur amount) and balanced N/P ratio (negative/positive electrode capacity) also need to be improved. Second, structure of as-prepared organosulfur materials and their charge storage mechanism has not been systematically investigated. Advanced characterization methods need to be developed and applied for the investigation of bonding patterns of sulfur such as S-S/C-S/C=S bonds in the complicated molecule structures as well as for the lithiation mechanism of these specific sites. Finally, improving the stability and electrochemical property of lithium metal anodes (LMAs) is another key factor. Organosulfur electrodes typically couple with LMAs, which has critical issues such as large volume expansion, dendritic and dead lithium formation as well as electrolyte consumption during electrochemical cycling. These issues should be taken seriously to enhance the overall performance of cells using organic sulfur cathodes. Therefore, several aspects for further research of organosulfur electrodes are suggested below.

4.1 Optimization of the electrochemical performance

As mentioned in the previous section, developing organic polymers with long sulfur chains and functional groups can significantly enhance the cyclic stability of organosulfur electrode materials. An ideal organosulfur electrode would have stable organic backbone with high sulfur content, higher electronic and ionic conductivity as well as compatibility toward electrolytes. Typically, higher active material loading is required for achieving high energy density. However, this would cause the increased thickness and porosity of the electrode and resulted in requiring large amount of electrolyte. Therefore, thick electrode architecture with optimized porosity and E/S ratio, as well as good wettability of electrolyte is needed. In terms of improving the kinetics, introduction of Se doping and/or conductive polymers are effective ways to facilitate Li^+ and electron transport, which can also significantly improve the utilization of active materials. Fabricating composite electrodes using CNTs or graphite can also improve the utilization of the active materials. Grafting organosulfur molecule with other electrochemically active organic species such as carbonyl groups, organic radicals and azo groups can potentially increase the energy density and improve the cyclic stability. Moreover, the structure of organosulfur compounds is rich in diversity and can be further modified by introducing different functional groups. The redox potential of organosulfur compounds can be tuned by the introducing of electron-withdrawing groups or electron-donating groups. These groups can adjust the energy level of lowest unoccupied molecular orbital (LUMO), which determines the redox potential. Typically, electron-withdrawing groups such as $-\text{Cl}$, $-\text{F}$, $-\text{Br}$, $-\text{NO}_2$, $-\text{CN}$ and $-\text{CF}_3$ can elevate the redox potential, while electron-donating groups such as $-\text{OH}$, $-\text{NH}_2$, $-\text{CH}_3$ and $-\text{OCH}_3$ lower the redox potential of the organosulfur compounds. In addition, the number of substituent groups can also affect the redox behavior of the organosulfur compounds. In terms of the cyclic stability, the introduction of high-polarity groups such as $-\text{COOM}$ and $-\text{OM}$ (M is alkali metals) can reduce the solubility of the electrode materials in the electrolyte and enhance their cyclic performances. For the practical applications, large-scale production of electrode materials using green and scalable manufacture process should be considered. To further increase the energy density of the organosulfur electrode materials and enhance their cyclic performance, future studies are needed on the following aspects: (1) designing organosulfur electrode materials with more redox-active sites and lower molecular weight to achieve higher capacity; (2) using more effective electron conducting agents to increase the utilization of the active materials; (3) modifying the molecular structure and introducing the electron-withdrawn groups to increase the working potential; (4) crosslinking small molecules to form polymers as well as increasing the polymerization degrees to reduce the solubility in electrolyte to enhance the cyclic stability; (5) introducing high-polarity organic groups or synthesizing carbon composites using CNTs, graphene and carbon foam to reduce the solubility in electrolyte; (6) combining organosulfur materials and inorganic nanomaterials to achieve stable cyclic performance and rate capability; (7) utilizing the multifunctional binders and modifying separators to enhance the cyclic stability; (8) optimizing the electrolyte, for example using high concentration or localized high concentration electrolytes, introducing electrolyte additives and developing quasi- or all-solid-state electrolytes to mitigate the dissolution issue.

4.2 Development of advanced characterization techniques

To further increase the specific capacity of the organosulfur cathodes there are several key factors that deserve more attentions: (1) How does the molecular structure of the organosulfur cathode determining the electrochemical performances? (2) What is the charge storage mechanism for those electrode materials with complex molecular structure? (3) How stable the sulfur is bonded to the organic backbone? (4) Does the designed special molecular structure can effectively suppress the polysulfide shuttling effect? The answers will provide valuable information for designing and synthesizing new organosulfur cathodes as well as improving their overall performance. The development of characterization techniques for structural and

mechanism studies of organic materials have been quite successful in providing new tools. For example, FT-IR analysis combined with NMR spectroscopy (^1H , ^7Li and ^{13}C) are widely used for determining the molecular structure since these techniques can directly identify various organic function groups. Raman spectroscopy provides information about other type of vibrational modes of the species and the identification of certain chemical bonds. The viability of Raman spectroscopy for detecting S-S bond in the organosulfur compounds has been demonstrated in previous studies. Moreover, XPS can precisely confirm the cleavage/recombination of the disulfide bonds. Unfortunately, the conventional XPS technique using lab x-ray source can only provide the information with limited probing depth (several nanometers). Therefore, it is essential to develop advanced characterization techniques which can provide comprehensive information about the charge storage mechanism and structure of organic sulfur electrode materials. Synchrotron-based x-ray techniques are powerful tools for studying structure evolution, charge storage mechanism as well as performance degradation mechanism of the electrode materials.^{125, 126} Although synchrotron x-ray techniques have been widely utilized for inorganic cathode material research, only limited studies have been reported on organic cathode materials. Therefore, introducing synchrotron-based x-ray techniques will help us to gain in-depth understanding of structure and redox mechanism of organic sulfur electrodes. X-ray absorption spectroscopy (XAS) is an elementally selective technique to probe the atomic arrangement and electronic structure of materials such as valence state and site symmetry of the absorbing atoms. Soft XAS technique (<3 KeV) has been applied to study the light elements such as C, N, O and S, which are the major elements in organic materials. A successful example was demonstrated by Shadik et al. in Yang's group,⁴⁶ revealing the charge compensation mechanism of TPQD organodisulfide cathode using S K-edge XAS as shown in Fig. 12a. In S K-edge XAS spectra, typical features of S=C π^* , S-S σ^* and S-C σ^* bonds are clearly distinguished. Based on the changes in the peak intensity, it can be concluded that S=C groups in TPQD are not involved in the charge storage process. The capacity is mainly attributed to the breakage and reformation of disulfide bonds during lithiation and delithiation process, respectively. Pair distribution function (PDF) analysis is another important characterization tool for understanding the structure evolution of organic materials especially for those having poor crystallinity. PDF, as a total scattering technique, including both Bragg scattering and diffuse scattering, has the capability to probe both crystalline phase and amorphous phase. The position of PDF peak corresponds to the bond length of atomic pair and the intensity relates to the relative abundance of these pairs.¹²⁷ As shown in Fig. 12b, lengths of S-S, C=O, C-S and C-C/C=C bonds in TPQD cathode are directly probed by PDF.⁴⁶ In addition, bonding pattern of sulfur in PTCDA-PAN-S composite and activation mechanism of this sulfur rich polymer are also studied using PDF.¹²⁸ Connection of sulfur with polymer backbone through C-S and O-S bonds as well as the existence of disulfide S-S bond in the pristine structure are proved by PDF data shown in Fig. 12c. More interestingly, breakage of some of S-O bonds and formation of more S-S bond during activation cycle are suggested based on the intensities of S-S and S-O peaks before and after cycling (Fig. 12d-f). These results demonstrated that advanced characterization techniques such as XAS and PDF can not only confirm the structure of as-prepared organic sulfur materials, but also provide direct evidence for lithiation mechanism. In addition, spatial resolved 2D x-ray fluorescence mapping combined with XAS spectra is a good way in mapping the sulfur species distribution visually together with their valence states, not only on the electrode but also in the electrolyte.¹²⁹

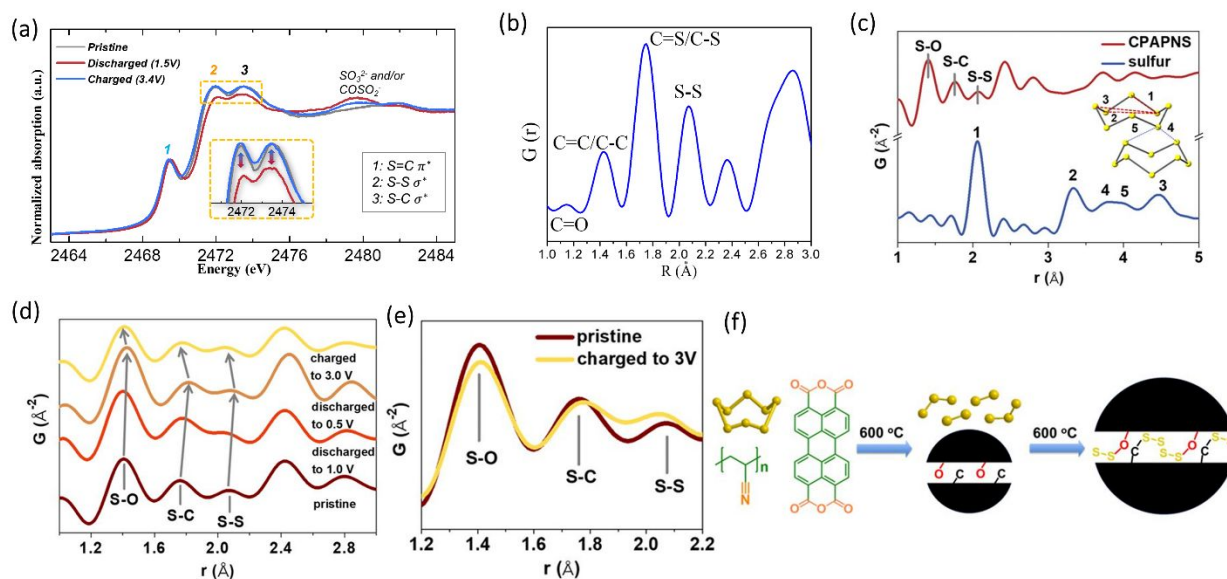


Figure 12. (a) S-K edge XAS spectra of TPQD electrodes at different state of charge. (b) PDF pattern of the as-prepared TPQD sample. Reproduced with permission.⁴⁶ Copyright 2019, Wiley-VCH. (c) PDF data of sulfur and CPAPN-S. Characteristic bonds and their corresponding PDF peaks are labeled. (d) PDF data of pristine and ex situ CPAPN-S electrodes in the first cycle, indicating that S-O, S-C, and S-S bond lengths generally increase during discharge and decrease during charge. (e) PDF data of charge-to-3 V electrode overlaid on the pristine data (without offset), showing the decrease of S-O peak and increase of S-S peak after first cycle. (f) A schematic illustration of the formation of chemical bonding stabilized carbon-small sulfur composite. Reproduced with permission.¹²⁸ Copyright 2020, National Academy of Sciences.

4.3 Stabilization of the LMAs

For the application of organosulfur materials in Li-S batteries, the stability of Li metal anode (LMA) also needs to be considered. Electrolyte modification such as optimization of the electrolyte components and introducing SEI formation additives can regulate the uniform nucleation of lithium and further suppress formation of dendritic lithium. Utilization of localized high concentration electrolyte (LHCE) is a promising approach to form stable SEI layer since a large number of anion can enter the solvation shell to form LiF-rich interface.¹³⁰ Soluble organosulfur compounds can also be used as film forming electrolyte additive to reduce the electrolyte reactivity toward the LMAs. It was also found that 3D composite LMAs not only suppress the volume expansion of Li metal but also reduce the uneven local current density of the electrode, resulting in homogeneous Li stripping/plating behaviors.^{131, 132}

Overall, molecular designing of organic sulfur electrode with high sulfur loading and stable structure, in-depth understanding of the relationship between structure and electrochemical performance as well as developing novel approaches to enable safe and stable operation are all important and more efforts are still needed in the future. These are essential to promote development of organosulfur materials for the next generation of rechargeable batteries.

Acknowledgement

This work was supported by the Assistant Secretary for Energy Efficiency and Renewable Energy, Vehicle Technology Office of the U.S. Department of Energy through the Advanced Battery Materials Research (BMR) Program, including Battery500 Consortium under contract DE-SC0012704.

Reference

1. J. B. Goodenough and Y. Kim, *Chem. Mater.*, 2010, **22**, 587-603.
2. D. Larcher and J. M. Tarascon, *Nat. Chem.*, 2015, **7**, 19-29.
3. Y. Lu and J. Chen, *Nat. Rev. Chem.*, 2020, **4**, 127-142.
4. Z. Song and H. Zhou, *Energy Environ. Sci.*, 2013, **6**, 2280-2301.
5. J. J. Shea and C. Luo, *ACS Appl. Mater. Interfaces* 2020, **12**, 5361-5380.
6. Y. Lu, Q. Zhang, L. Li, Z. Niu and J. Chen, *Chem*, 2018, **4**, 2786-2813.
7. Y. Liang and Y. Yao, *Joule*, 2018, **2**, 1690-1706.
8. J. Gao, M. A. Lowe, S. Conte, S. E. Burkhart and H. D. Abruna, *Chem. Eur. J.*, 2012, **18**, 8521-8526.
9. L. Liu, F. Tian, X. Wang, Z. Yang, M. Zhou and X. Wang, *React. Funct. Polym.*, 2012, **72**, 45-49.
10. L. M. Zhu, A. W. Lei, Y. L. Cao, X. P. Ai and H. X. Yang, *Chem. Commun.*, 2013, **49**, 567-569.
11. K. Nakahara, S. Iwasa, M. Satoh, Y. Morioka, J. Iriyama, M. Suguro and E. Hasegawa, *Chem. Phys. Lett.*, 2002, **359**, 351-354.
12. Z. Song, H. Zhan and Y. Zhou, *Chem. Commun.*, 2009, DOI: 10.1039/b814515f, 448-450.
13. C. Luo, O. Borodin, X. Ji, S. Hou, K. J. Gaskell, X. Fan, J. Chen, T. Deng, R. Wang, J. Jiang and C. Wang, *Proc. Natl. Acad. Sci. U. S. A.*, 2018, **115**, 2004-2009.
14. D. Y. Wang, W. Guo and Y. Fu, *Acc. Chem. Res.*, 2019, **52**, 2290-2300.
15. X. Zhang, K. Chen, Z. Sun, G. Hu, R. Xiao, H.-M. Cheng and F. Li, *Energy Environ. Sci.*, 2020, **13**, 1076-1095.
16. J. Liu, M. Wang, N. Xu, T. Qian and C. Yan, *Energy Storage Mater.*, 2018, **15**, 53-64.
17. S.-H. Chung, C.-H. Chang and A. Manthiram, *Adv. Funct. Mater.*, 2018, **28**, 1801188.
18. Z. W. Seh, Y. Sun, Q. Zhang and Y. Cui, *Chem. Soc. Rev.*, 2016, **45**, 5605-5634.
19. X. Fang and H. Peng, *Small*, 2015, **11**, 1488-1511.
20. W. Wang, Z. Cao, G. A. Elia, Y. Wu, W. Wahyudi, E. Abou-Hamad, A.-H. Emwas, L. Cavallo, L.-J. Li and J. Ming, *ACS Energy Lett.*, 2018, **3**, 2899-2907.
21. S. Chen, F. Dai, M. L. Gordin, Z. Yu, Y. Gao, J. Song and D. Wang, *Angew. Chem. Int. Ed.*, 2016, **55**, 4231-4235.
22. S. J. Visco, *J. Electrochem. Soc.*, 1988, **135**, 2905.
23. S. J. Visco, *J. Electrochem. Soc.*, 1989, **136**, 661.
24. S. J. Visco, *J. Electrochem. Soc.*, 1990, **137**, 1191.
25. T. Inamasu, D. Yoshitoku, Y. Sumi-otorii, H. Tani and N. Ono, *J. Electrochem. Soc.*, 2003, **150**, A128-A132.
26. A. Bhargava, S. V. Patil and Y. Fu, *Sustain. Energy Fuels*, 2017, **1**, 1007-1012.
27. D.-Y. Wang, Y. Si, J. Li and Y. Fu, *J. Mater. Chem. A*, 2019, **7**, 7423-7429.
28. Y. Liang, Z. Tao and J. Chen, *Adv. Energy Mater.*, 2012, **2**, 742-769.
29. L. J. Xue, J. X. Li, S. Q. Hu, M. X. Zhang, Y. H. Zhou and C. M. Zhan, *Electrochem. Commun.*, 2003, **5**, 903-906.
30. Y. Li, H. Zhan, L. Kong, C. Zhan and Y. Zhou, *Electrochem. Commun.*, 2007, **9**, 1217-1221.
31. M. Liu, *J. Electrochem. Soc.*, 1989, **136**, 2570.
32. M. Liu, *J. Electrochem. Soc.*, 1990, **137**, 750.
33. M. Liu, *J. Electrochem. Soc.*, 1991, **138**, 1891.
34. M. M. Doeff, *J. Electrochem. Soc.*, 1992, **139**, 2077.

35. T. Sotomura, H. Uemachi, K. Takeyama, K. Naoi and N. Oyama, *Electrochim. Acta*, 1992, **37**, 1851-1854.
36. N. Oyama, T. Tatsuma, T. Sato and T. Sotomura, *Nature*, 1995, **373**, 598-600.
37. J. Li, H. Zhan and Y. Zhou, *Electrochem. Commun.*, 2003, **5**, 555-560.
38. Y. Kiya, A. Iwata, T. Sarukawa, J. C. Henderson and H. D. Abruña, *J. Power Sources*, 2007, **173**, 522-530.
39. Y. Kiya, G. R. Hutchison, J. C. Henderson, T. Sarukawa, O. Hatozaki, N. Oyama and H. D. Abruña, *Langmuir*, 2006, **22**, 10554-10563.
40. H. Tsutsumi and K. Fujita, *Electrochim. Acta*, 1995, **40**, 879-882.
41. H. Tsutsumi, K. Okada and T. Oishi, *Electrochim. Acta*, 1996, **41**, 2657-2659.
42. K. Naoi, *J. Electrochem. Soc.*, 1997, **144**, L173.
43. S.-R. Deng, L.-B. Kong, G.-Q. Hu, T. Wu, D. Li, Y.-H. Zhou and Z.-Y. Li, *Electrochim. Acta*, 2006, **51**, 2589-2593.
44. T. Sarukawa and N. Oyama, *J. Electrochem. Soc.*, 2010, **157**, F23-F29.
45. M. B. Preefer, B. Oschmann, C. J. Hawker, R. Seshadri and F. Wudl, *Angew. Chem. Int. Ed.*, 2017, **56**, 15118-15122.
46. Z. Shadike, H. S. Lee, C. Tian, K. Sun, L. Song, E. Hu, I. Waluyo, A. Hunt, S. Ghose, Y. Hu, J. Zhou, J. Wang, P. Northrup, S. M. Bak and X. Q. Yang, *Adv. Energy Mater.*, 2019, **9**, 1900705.
47. K. Naoi, *J. Electrochem. Soc.*, 1997, **144**, L170.
48. M. Wu, Y. Cui, A. Bhargav, Y. Losovyj, A. Siegel, M. Agarwal, Y. Ma and Y. Fu, *Angew. Chem. Int. Ed.*, 2016, **55**, 10027-10031.
49. M. Wu, A. Bhargav, Y. Cui, A. Siegel, M. Agarwal, Y. Ma and Y. Fu, *ACS Energy Lett.*, 2016, **1**, 1221-1226.
50. W. Guo, Z. D. Wawrzyniakowski, M. M. Cerda, A. Bhargav, M. D. Pluth, Y. Ma and Y. Fu, *Chem. Eur. J.*, 2017, **23**, 16941-16947.
51. J. Zhao, Y. Si, Z. Han, J. Li, W. Guo and Y. Fu, *Angew. Chem. Int. Ed.*, 2020, **59**, 2654-2658.
52. G. Weng, Y. Su, Z. Liu, J. Zhang, W. Dong and C. Xu, *Energy*, 2009, **34**, 1351-1354.
53. H. Tsutsumi, Y. Oyari, K. Onimura and T. Oishi, *J. Power Sources*, 2001, **92**, 228-233.
54. Y.-Z. Su, W. Dong, J.-H. Zhang, J.-H. Song, Y.-H. Zhang and K.-C. Gong, *Polymer*, 2007, **48**, 165-173.
55. M. Amaike and T. Iihama, *Synth. Met.*, 2006, **156**, 239-243.
56. H. Uemachi, Y. Iwasa and T. Mitani, *Chem. Lett.*, 2000, **29**, 946-947.
57. J. Li, H. Zhan, L. Zhou, S. Deng, Z. Li and Y. Zhou, *Electrochem. Commun.*, 2004, **6**, 515-519.
58. H. Uemachi, Y. Iwasa and T. Mitani, *Electrochim. Acta*, 2001, **46**, 2305-2312.
59. X.-g. Yu, J.-y. Xie, J. Yang, H.-j. Huang, K. Wang and Z.-s. Wen, *J. Electroanal. Chem.*, 2004, **573**, 121-128.
60. P. Krishnan, S. G. Advani and A. K. Prasad, *J. Power Sources*, 2011, **196**, 7755-7759.
61. S.-c. Zhang, L. Zhang, W.-k. Wang and W.-j. Xue, *Synth. Met.*, 2010, **160**, 2041-2044.
62. J. Wang, J. Yang, J. Xie and N. Xu, *Adv. Mater.*, 2002, **14**, 963-965.
63. J. Wang, J. Yang, C. Wan, K. Du, J. Xie and N. Xu, *Adv. Funct. Mater.*, 2003, **13**, 487-492.
64. J. Wang, Y. Wang, X. He, J. Ren, C. Jiang and C. Wan, *J. Power Sources*, 2004, **138**, 271-273.
65. X. Yu, J. Xie, Y. Li, H. Huang, C. Lai and K. Wang, *J. Power Sources*, 2005, **146**, 335-339.
66. J. Fanous, M. Wegner, J. Grimminger, Å. Andresen and M. R. Buchmeiser, *Chem. Mater.*, 2011, **23**, 5024-5028.
67. X. Xing, Y. Li, X. Wang, V. Petrova, H. Liu and P. Liu, *Energy Storage Mater.*, 2019, **21**, 474-480.
68. X. Chen, L. Peng, L. Wang, J. Yang, Z. Hao, J. Xiang, K. Yuan, Y. Huang, B. Shan, L. Yuan and J. Xie, *Nat. Commun.*, 2019, **10**, 1021.
69. J. Wang, L. Yin, H. Jia, H. Yu, Y. He, J. Yang and C. W. Monroe, *ChemSusChem*, 2014, **7**, 563-569.

70. L. Yin, J. Wang, J. Yang and Y. Nuli, *J. Mater. Chem.*, 2011, **21**, 6807–6810.
71. J. Y. Zhang, L. B. Kong, L. Z. Zhan, J. Tang, H. Zhan, Y. H. Zhou and C. M. Zhan, *J. Power Sources*, 2007, **168**, 278-281.
72. J. Tang, Z.-P. Song, N. Shan, L.-Z. Zhan, J.-Y. Zhang, H. Zhan, Y.-H. Zhou and C.-M. Zhan, *J. Power Sources*, 2008, **185**, 1434-1438.
73. L. Zhan, Z. Song, N. Shan, J. Zhang, J. Tang, H. Zhan, Y. Zhou, Z. Li and C. Zhan, *J. Power Sources*, 2009, **193**, 859-863.
74. J. Zhang, L. Kong, L. Zhan, J. Tang, H. Zhan, Y. Zhou and C. Zhan, *Electrochem. Commun.*, 2008, **10**, 1551-1554.
75. T. P. Vaid, M. E. Easton and R. D. Rogers, *Synth. Met.*, 2017, **231**, 44-50.
76. J. Ren, X. Wang, H. Liu, Y. Hu, X. Zhang and T. Masuda, *React. Funct. Polym.*, 2020, **146**, 104365.
77. J. Tang, L. Kong, J. Zhang, L. Zhan, H. Zhan, Y. Zhou and C. Zhan, *React. Funct. Polym.*, 2008, **68**, 1408-1413.
78. D. Canevet, M. Salle, G. Zhang, D. Zhang and D. Zhu, *Chem. Commun.*, 2009, 2245-2269.
79. Y. Inatomi, N. Hojo, T. Yamamoto, S.-i. Watanabe and Y. Misaki, *ChemPlusChem*, 2012, **77**, 973-976.
80. S. Iwamoto, Y. Inatomi, D. Ogi, S. Shibayama, Y. Murakami, M. Kato, K. Takahashi, K. Tanaka, N. Hojo and Y. Misaki, *Beilstein J. Org. Chem.*, 2015, **11**, 1136-1147.
81. M. Kato, K.-i. Senoo, M. Yao and Y. Misaki, *J. Mater. Chem. A*, 2014, **2**, 6747–6754.
82. W. J. Chung, J. J. Griebel, E. T. Kim, H. Yoon, A. G. Simmonds, H. J. Ji, P. T. Dirlam, R. S. Glass, J. J. Wie, N. A. Nguyen, B. W. Guralnick, J. Park, A. Somogyi, P. Theato, M. E. Mackay, Y. E. Sung, K. Char and J. Pyun, *Nat. Chem.*, 2013, **5**, 518-524.
83. A. G. Simmonds, J. J. Griebel, J. Park, K. R. Kim, W. J. Chung, V. P. Oleshko, J. Kim, E. T. Kim, R. S. Glass, C. L. Soles, Y.-E. Sung, K. Char and J. Pyun, *ACS Macro Lett.*, 2014, **3**, 229-232.
84. S. N. Talapaneni, T. H. Hwang, S. H. Je, O. Buyukcakir, J. W. Choi and A. Coskun, *Angew. Chem. Int. Ed.*, 2016, **55**, 3106-3111.
85. S. H. Je, H. J. Kim, J. Kim, J. W. Choi and A. Coskun, *Adv. Funct. Mater.*, 2017, **27**, 1703947.
86. S. H. Je, T. H. Hwang, S. N. Talapaneni, O. Buyukcakir, H. J. Kim, J.-S. Yu, S.-G. Woo, M. C. Jang, B. K. Son, A. Coskun and J. W. Choi, *ACS Energy Lett.*, 2016, **1**, 566-572.
87. I. Gomez, D. Mantione, O. Leonet, J. A. Blazquez and D. Mecerreyes, *ChemElectroChem*, 2018, **5**, 260-265.
88. X. Liu, Y. Lu, Q. Zeng, P. Chen, Z. Li, X. Wen, W. Wen, Z. Li and L. Zhang, *ChemSusChem*, 2020, **13**, 715-723.
89. F. Xu, S. Yang, G. Jiang, Q. Ye, B. Wei and H. Wang, *ACS Appl. Mater. Interfaces*, 2017, **9**, 37731-37738.
90. P. Dong, K. S. Han, J. I. Lee, X. Zhang, Y. Cha and M. K. Song, *ACS Appl. Mater. Interfaces*, 2018, **10**, 29565-29573.
91. I. Gracia, H. Ben Youcef, X. Judez, U. Oteo, H. Zhang, C. Li, L. M. Rodriguez-Martinez and M. Armand, *J. Power Sources*, 2018, **390**, 148-152.
92. H. Xu, Y. Shi, S. Yang and B. Li, *J. Power Sources*, 2019, **430**, 210-217.
93. H. Hu, B. Zhao, H. Cheng, S. Dai, N. Kane, Y. Yu and M. Liu, *Nano Energy*, 2019, **57**, 635-643.
94. S. Zeng, L. Li, D. Zhao, J. Liu, W. Niu, N. Wang and S. Chen, *J. Phys. Chem. C* 2017, **121**, 2495-2503.
95. B. Ding, Z. Chang, G. Xu, P. Nie, J. Wang, J. Pan, H. Dou and X. Zhang, *ACS Appl. Mater. Interfaces*, 2015, **7**, 11165-11171.
96. C.-H. Chang and A. Manthiram, *ACS Energy Lett.*, 2017, **3**, 72-77.
97. S. Zeng, L. Li, L. Xie, D. Zhao, N. Zhou, N. Wang and S. Chen, *Carbon*, 2017, **122**, 106-113.

98. F. Wu, S. Chen, V. Srot, Y. Huang, S. K. Sinha, P. A. van Aken, J. Maier and Y. Yu, *Adv. Mater.*, 2018, **30**, e1706643.
99. S. Zeng, L. Li, L. Xie, D. Zhao, N. Wang and S. Chen, *ChemSusChem*, 2017, **10**, 3378-3386.
100. D. Y. Wang, Y. Si, W. Guo and Y. Fu, *Adv. Sci.*, 2020, **7**, 1902646.
101. H. Kang, H. Kim and M. J. Park, *Adv. Energy Mater.*, 2018, **8**, 1802423.
102. H. Kim, J. Lee, H. Ahn, O. Kim and M. J. Park, *Nat. Commun.*, 2015, **6**, 7278.
103. B. A. Trofimov, M. V. Markova, L. V. Morozova, G. F. Prozorova, S. A. Korzhova, M. D. Cho, V. V. Annenkov and A. b. I. Mikhaleva, *Electrochim. Acta*, 2011, **56**, 2458-2463.
104. S. Chen, Y. Gao, Z. Yu, M. L. Gordin, J. Song and D. Wang, *Nano Energy*, 2017, **31**, 418-423.
105. S. Chen, D. Wang, Y. Zhao and D. Wang, *Small Methods*, 2018, **2**, 1800038.
106. S. Gu, J. Jin, S. Zhuo, R. Qian and Z. Wen, *ChemElectroChem*, 2018, **5**, 1717-1723.
107. J. Zhang, B. Sun, Y. Zhao, K. Kretschmer and G. Wang, *Angew. Chem. Int. Ed.*, 2017, **56**, 8505-8509.
108. G. Li, Y. Gao, X. He, Q. Huang, S. Chen, S. H. Kim and D. Wang, *Nat. Commun.*, 2017, **8**, 850.
109. G. Li, Q. Huang, X. He, Y. Gao, D. Wang, S. H. Kim and D. Wang, *ACS Nano*, 2018, **12**, 1500-1507.
110. R. Xu, X.-B. Cheng, C. Yan, X.-Q. Zhang, Y. Xiao, C.-Z. Zhao, J.-Q. Huang and Q. Zhang, *Matter*, 2019, **1**, 317-344.
111. Y. Zhao, G. Li, Y. Gao, D. Wang, Q. Huang and D. Wang, *ACS Energy Lett.*, 2019, **4**, 1271-1278.
112. W. Wang, F. Hao and P. P. Mukherjee, *ACS Appl. Mater. Interfaces*, 2020, **12**, 556-566.
113. B. Boateng, Y. Han, C. Zhen, G. Zeng, N. Chen, D. Chen, C. Feng, J. Han, J. Xiong, X. Duan and W. He, *Nano Lett.*, 2020, **20**, 2594-2601.
114. K.-S. Lee, Y.-K. Sun, J. Noh, K. S. Song and D.-W. Kim, *Electrochem. Commun.*, 2009, **11**, 1900-1903.
115. L. Xia, Y. Xia and Z. Liu, *Electrochim. Acta*, 2015, **151**, 429-436.
116. A. Abouimrane, S. A. Odom, H. Tavassol, M. V. Schulmerich, H. Wu, R. Bhargava, A. A. Gewirth, J. S. Moore and K. Amine, *J. Electrochem. Soc.*, 2012, **160**, A268-A271.
117. H. Gao, F. Maglia, P. Lamp, K. Amine and Z. Chen, *ACS Appl. Mater. Interfaces*, 2017, **9**, 44542-44549.
118. G.-L. Xu, Q. Liu, K. K. S. Lau, Y. Liu, X. Liu, H. Gao, X. Zhou, M. Zhuang, Y. Ren, J. Li, M. Shao, M. Ouyang, F. Pan, Z. Chen, K. Amine and G. Chen, *Nat. Energy*, 2019, **4**, 484-494.
119. Y. Sun, J. Huang, H. Xiang, X. Liang, Y. Feng and Y. Yu, *J. Mater. Sci. Technol.*, 2020, **55**, 198-202.
120. W. Li, Q. Zhang, G. Zheng, Z. W. Seh, H. Yao and Y. Cui, *Nano Lett.*, 2013, **13**, 5534-5540.
121. J. Pan, G. Xu, B. Ding, Z. Chang, A. Wang, H. Dou and X. Zhang, *RSC Adv.*, 2016, **6**, 40650-40655.
122. M. Zhang, Q. Meng, A. Ahmad, L. Mao, W. Yan and Z. Wei, *J. Mater. Chem. A*, 2017, **5**, 17647-17652.
123. L. Yan, X. Gao, J. P. Thomas, J. Ngai, H. Altounian, K. T. Leung, Y. Meng and Y. Li, *Sustain. Energy Fuels*, 2018, **2**, 1574-1581.
124. F.-L. Zeng, N. Li, Y.-Q. Shen, X.-Y. Zhou, Z.-Q. Jin, N.-Y. Yuan, J.-N. Ding, A.-B. Wang, W.-K. Wang and Y.-S. Yang, *Energy Storage Mater.*, 2019, **18**, 190-198.
125. Z. Shadike, E. Zhao, Y.-N. Zhou, X. Yu, Y. Yang, E. Hu, S. Bak, L. Gu and X.-Q. Yang, *Adv. Energy Mater.*, 2018, **8**, 1702588.
126. D. Liu, Z. Shadike, R. Lin, K. Qian, H. Li, K. Li, S. Wang, Q. Yu, M. Liu, S. Ganapathy, X. Qin, Q. H. Yang, M. Wagemaker, F. Kang, X. Q. Yang and B. Li, *Adv. Mater.*, 2019, **31**, e1806620.
127. X. Wang, S. Tan, X.-Q. Yang and E. Hu, *Chin. Phys. B*, 2020, **29**, 028802.
128. C. Luo, E. Hu, K. J. Gaskell, X. Fan, T. Gao, C. Cui, S. Ghose, X. Q. Yang and C. Wang, *Proc. Natl. Acad. Sci. U. S. A.*, 2020, **117**, 14712-14720.
129. X. Yu, H. Pan, Y. Zhou, P. Northrup, J. Xiao, S. Bak, M. Liu, K.-W. Nam, D. Qu, J. Liu, T. Wu and X.-Q. Yang, *Adv. Energy Mater.*, 2015, **5**, 1500072.

130. J. Liu, Z. Bao, Y. Cui, E. J. Dufek, J. B. Goodenough, P. Khalifah, Q. Li, B. Y. Liaw, P. Liu, A. Manthiram, Y. S. Meng, V. R. Subramanian, M. F. Toney, V. V. Viswanathan, M. S. Whittingham, J. Xiao, W. Xu, J. Yang, X.-Q. Yang and J.-G. Zhang, *Nat. Energy*, 2019, **4**, 180-186.
131. X.-Y. Yue, X.-L. Li, W.-W. Wang, D. Chen, Q.-Q. Qiu, Q.-C. Wang, X.-J. Wu, Z.-W. Fu, Z. Shadike, X.-Q. Yang and Y.-N. Zhou, *Nano Energy*, 2019, **60**, 257-266.
132. X.-Y. Yue, W.-W. Wang, Q.-C. Wang, J.-K. Meng, Z.-Q. Zhang, X.-J. Wu, X.-Q. Yang and Y.-N. Zhou, *Energy Storage Mater.*, 2018, **14**, 335-344.

Table of Contents

Lithium storage properties of organosulfur electrodes including organodisulfide, thioethers, organosulfide polymers and sulfurized polyacrylonitrile have been comprehensively reviewed.

